

CHAPTER 4

RESULTS AND DISCUSSION

4.1 Anatomical comparison between normal and chilling injured longan fruit pericarps cv. Daw and Biew Kiew

4.1.1 The anatomy of normal longan fruit pericarp

4.1.1.1 Visual observation of longan fruit pericarp

The longan fruit cv. Daw was compressed round and lob-sided with thick skin and rather tough. The outer surface of pericarps were quite rough with a number of brown patches and yellowish brown color (**Figure 4.1 A**). The longan fruit cv. Biew Kiew was rather large, compressed round, very lop-sided and the pericarp was brownish green color (**Figure 4.1 B**).

4.1.1.2 Stereomicroscope observation of longan fruit pericarp

Stereomicroscope observation of longan pericarp showed brown nodule (warty), brown patches and groups of trichomes around the nodules (**Figure 4.1 C**). The inner surface of fruit pericarp was a waxy with creamy white color and with clearly visible network of vascular strands (**Figure 4.1 D**).

4.1.1.3 Microscopic anatomy and ultrastructure of longan fruit pericarp

The anatomy of normal longan fruit pericarps from cv. Daw and Biew Kiew were different in pericarp thickness but similar in ultrastructure. When the outer pericarp of longan fruit was assessed with SEM, it was found that the surface was covered by a thin discontinuous cuticle layer. There are many natural crackings on the fruit pericarp surface (**Figure 4.2 A**). Few stomata and some groups of trichomes were also observed on the pericarp surface (**Figures 4.2 B-D**). Trichome structure on longan fruit pericarp was 2-celled trichome and formed from both epidermal and subepidermal tissues when the trichome was assessed with LM (**Figures 4.2 E-F**). Structurally, the trichome may be subdivided into unicellular and multicellular (Esau,

1953). Types of surface and underlying tissues of fruits and vegetables have a marked effect on the rate of water loss. The resulting water loss, causes formations of a dry epidermal layer (Chen *et al.*, 1998).

The transverse section of longan fruit pericarp was revealed a pericarp thickness in cv. Daw of about 518-644 μm (average 575 μm) (**Figure 4.3 A**) and about 475-630 μm (average 552 μm) for cv. Biew Kiew (**Figure 4.3 B**), respectively. The LM observation revealed that the pericarps of both cultivars had similar structure and consisted of three layers. The layers differed by cell type, shape and arrangement (**Figures 4.3 C-D** and **4.4**).

A. Exocarp

The exocarp consisted of a thin discontinuous cuticle covered on the epidermal layer (**Figures 4.5 A-B**), under which there were 2-3 layers of small rectangular cells in the subepidermis (**Figure 4.5 C**). These microscopic observations imply that rapid moisture loss from longan fruit may be related to water vapor moves to the outside atmosphere through lenticels, stomata, natural openings, injured areas or directly through the cuticle. Longan fruit rapidly lost moisture once harvested. The majority of initial loss derived from cracked pericarp.

B. Mesocarp

The mesocarp thickness was about 70% of the total pericarp thickness. It was found that the various cell sizes and shapes were rather round and elliptical with thick cell walls, large intercellular spaces between adjacent cells, and contained vascular tissue and some stone cells (**Figure 4.4**). Stone cells occurred in small groups with close arrangement and exhibited a bluish green color when they viewed with LM (Figure 4.6 A). The ultrastructure of stone cells contained a thick secondary cell wall when they were viewed with TEM (Figure 4.6 B). The stone cell structure was stubbled with a thick secondary wall, which lacked protoplasts (Starr, 2004). The parenchyma cells in the mesocarp contained intact plasmalemma tightly appressed to the walls, a thin layer of peripheral cytoplasm, and an intact tonoplast (**Figures 4.6 C-F**). They were rather round shape (**Figures 4.6 C-D**) and elliptical shape cells (**Figures 4.6 E-F**) when

observed by TEM, contained many vacuoles and cell organelles. The middle lamella was visible as relatively electron dense region between the primary walls. The cells were largely vacuolated with cytoplasm confined to a narrow layer adjacent to the cell wall (**Figure 4.6 D**). Vascular tissues were observed clearly in the lower mesocarp layer (**Figure 4.7 A**). The xylem vessels were tubular with helical, thick secondary walls and consisted of one layer cell (**Figures 4.7 B-D**). In addition, the mesocarp cells contained large intercellular spaces between adjacent cells.

C. Endocarp

The endocarp was made up of a square shaped cells in a single layer with thick cell walls (**Figure 4.8 A**). The cells were largely vacuolated with cytoplasm confined to a narrow layer adjacent to the cell wall. No organelles were evident in these cells under TEM observation (**Figure 4.8 B**).

4.1.1.4 Anatomy of inner surface longan fruit pericarp

The inner surface of pericarp was a waxy with creamy white color and with clearly visible network vascular strands (**Figure 4.9 A**). However, when the inner side of pericarp was viewed with SEM it exhibited a slight curve (**Figure 4.9 B**). Additionally, when the inner side of pericarp (creamy white and shiny) was peeled off (**Figure 4.9 C**). It was exhibited a network of connecting tubes, via stellate arms to adjacent cells with large intercellular spaces (**Figures 4.9 D-F**).

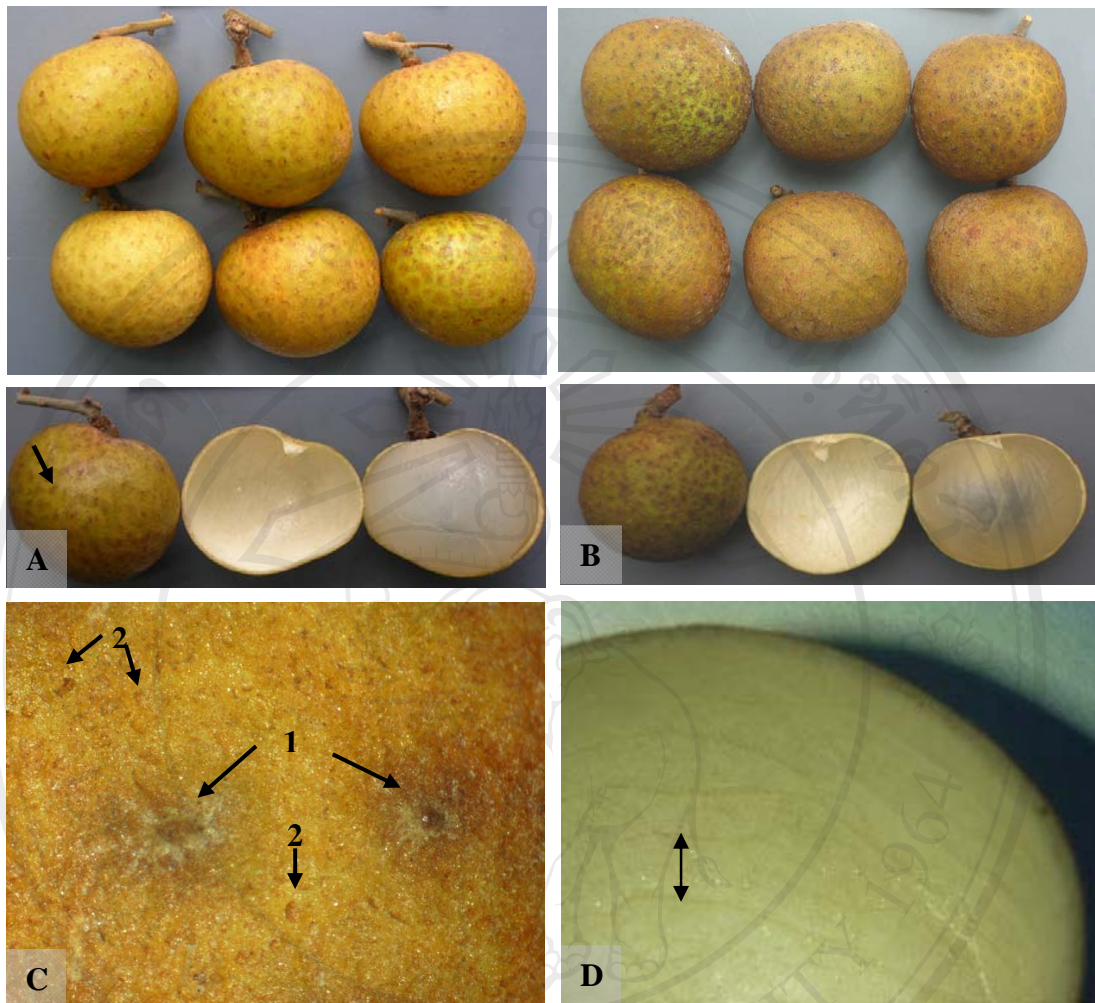


Figure 4.1 The longan fruits cv. Daw and Biew Kiew after harvest.

A = Longan fruit cv. Daw

B = Longan fruit cv. Biew Kiew

C = Stereomicrographs of the outer pericarp surface (Mag. $\times 4$)

D = Stereomicrographs of inner pericarp surface showed the waxy with creamy white color (Mag. $\times 4$)

1 = Brown nodules scattered on the outer pericarp surface

2 = Brown patches scattered on the outer pericarp surface

\longleftrightarrow = Vascular strands on the inner pericarp surface

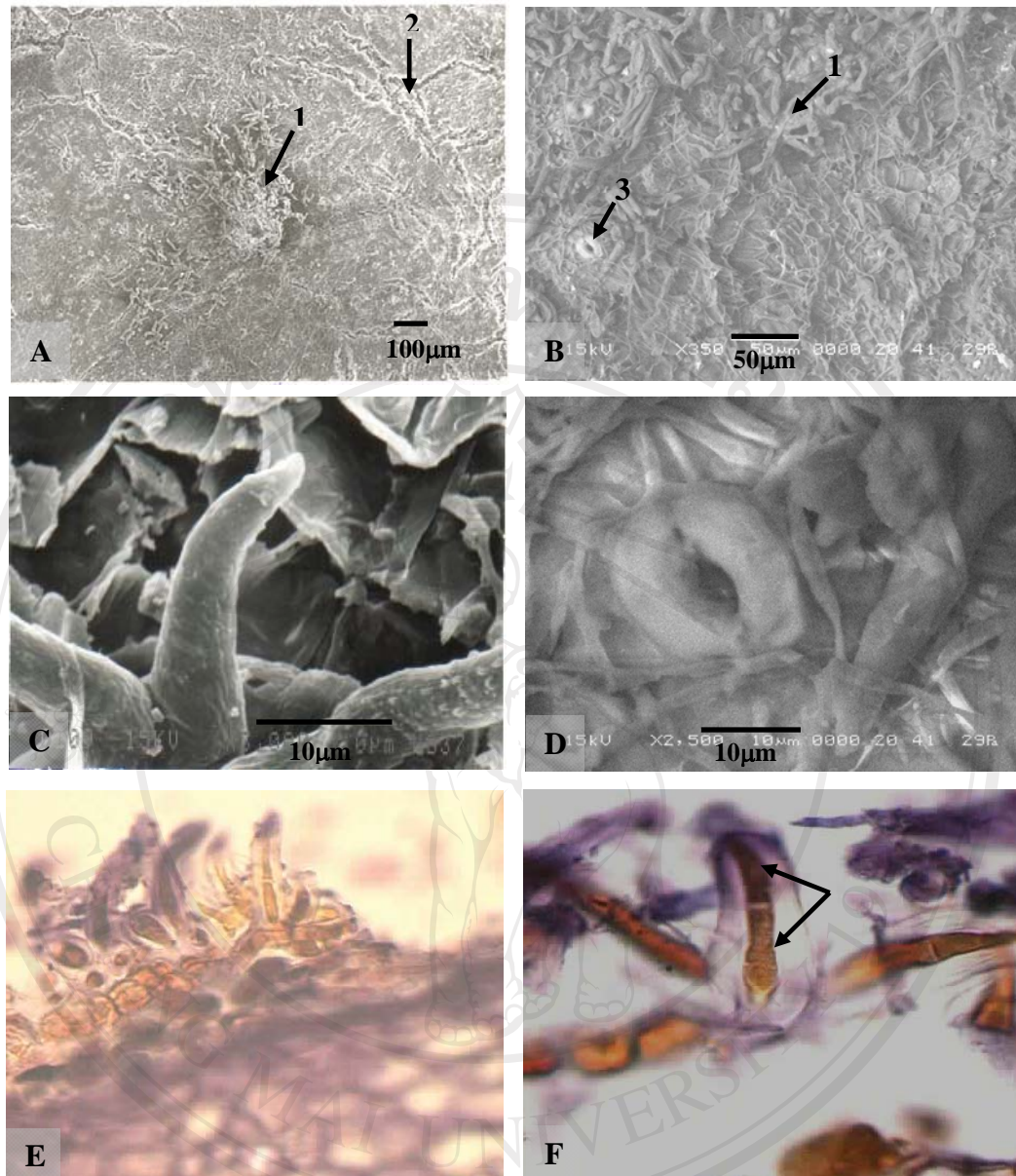


Figure 4.2 SEM and LM micrographs of the outer longan fruit pericarp surface.

A = Outer pericarp surface showing a group of trichomes and natural openings (Mag. $\times 70$)

B = Groups of trichomes and stomata were covered on the outer pericarp surface (Mag. $\times 350$)

C = SEM micrograph of trichome (Mag. $\times 3,000$)

D = SEM micrograph of stomata (Mag. $\times 2,500$)

E = LM micrograph of trichomes on the pericarp surface (Mag. $\times 40$)

F = LM micrograph of trichomes was made up of 2-celled trichomes structure (arrows head) (Mag. $\times 100$)

1 = group of trichomes, 2 = natural opening, 3 = stomata

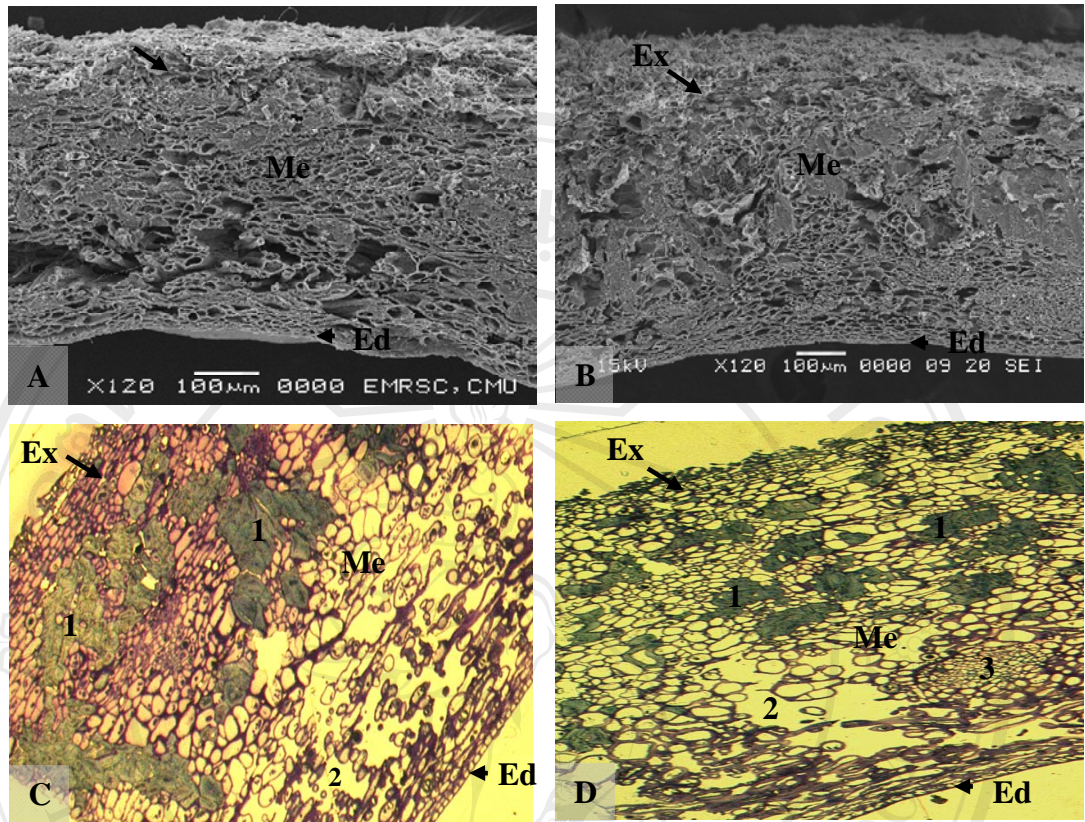


Figure 4.3 Transverse section micrographs of normal longan fruit pericarp cv. Daw (left) and Biew Kiew (right).

A = SEM micrograph of longan pericarp cv. Daw (Mag. $\times 120$)

B = SEM micrograph of longan pericarp cv. Biew Kiew (Mag. $\times 120$)

C = LM micrograph of longan pericarp cv. Daw (Mag. $\times 10$)

D = LM micrograph of longan pericarp cv. Biew Kiew (Mag. $\times 10$)

1 = stone cell, 2 = intercellular space, 3 = vascular tissue

Ex = exocarp, Me = mesocarp, Ed = endocarp

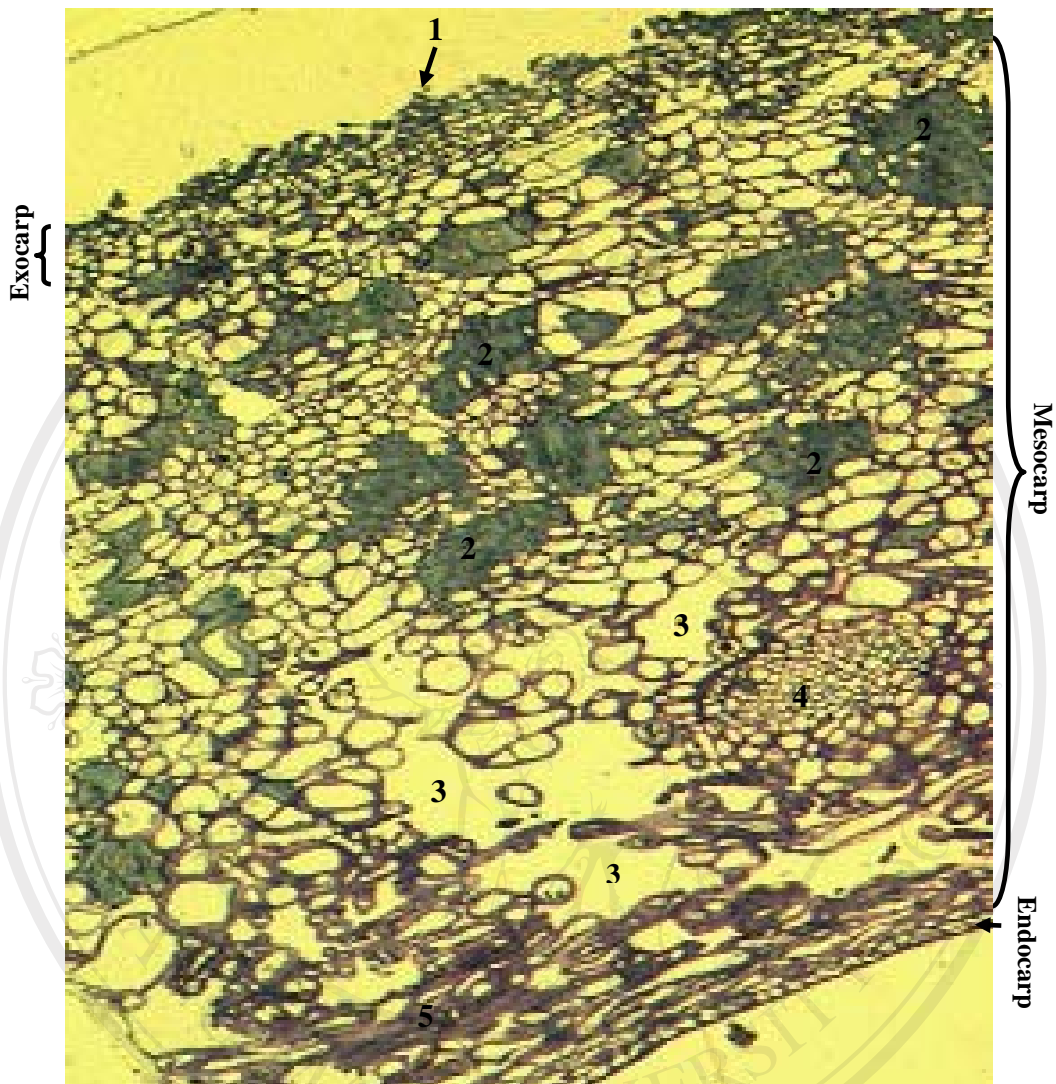


Figure 4.4 Transverse section micrograph of normal longan fruit pericarp cv. Biew Kiew consist of three layers; exocarp, mesocarp, and endocarp.

1 = cuticle layer, 2 = stone cell, 3 = intercellular space

4 = vascular tissue, 5 = elliptical shape cell with thick cell wall

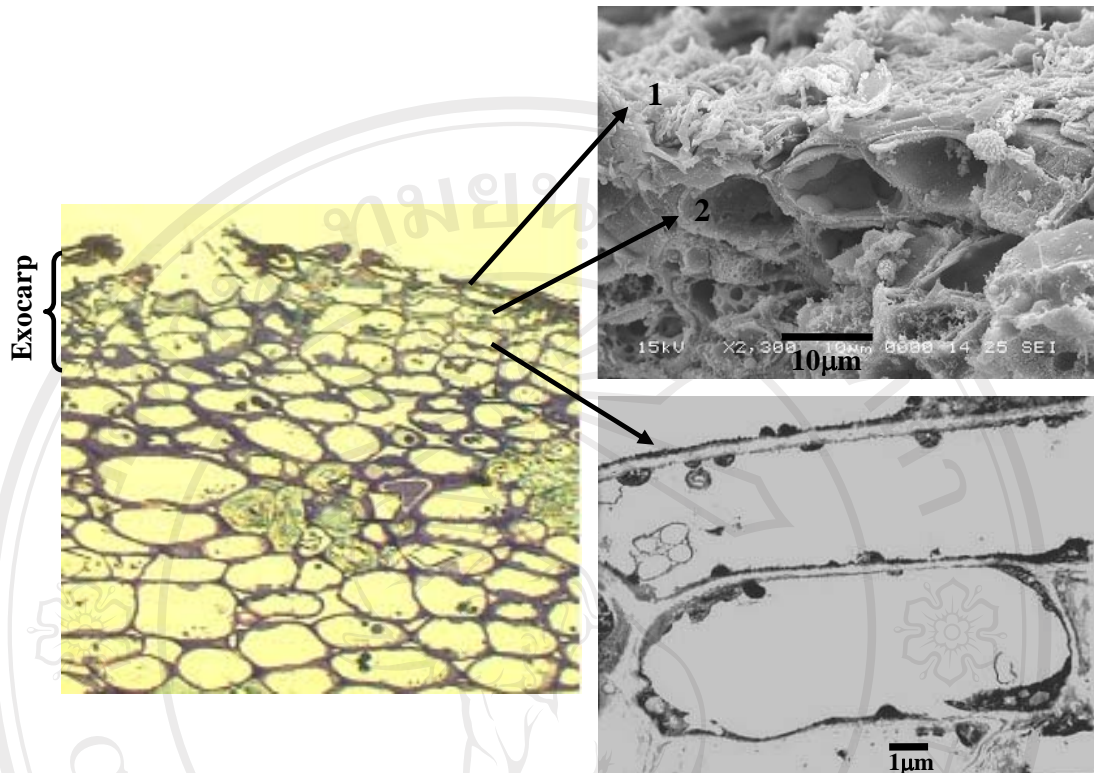


Figure 4.5 Transverse section micrographs of exocarp layer.

A = LM micrograph of exocarp layer was consisted of cuticle layer, epidermal layer and 2-3 of small rectangular cell layer (Mag. $\times 40$)

B = SEM micrograph of exocarp showing cuticle and epidermal layers (Mag. $\times 2,300$)

C = TEM micrograph of 2-3 of small rectangular cell layer deep in the subepidermis (Mag. $\times 5,000$)

1 = cuticle layer, 2 = epidermal layer

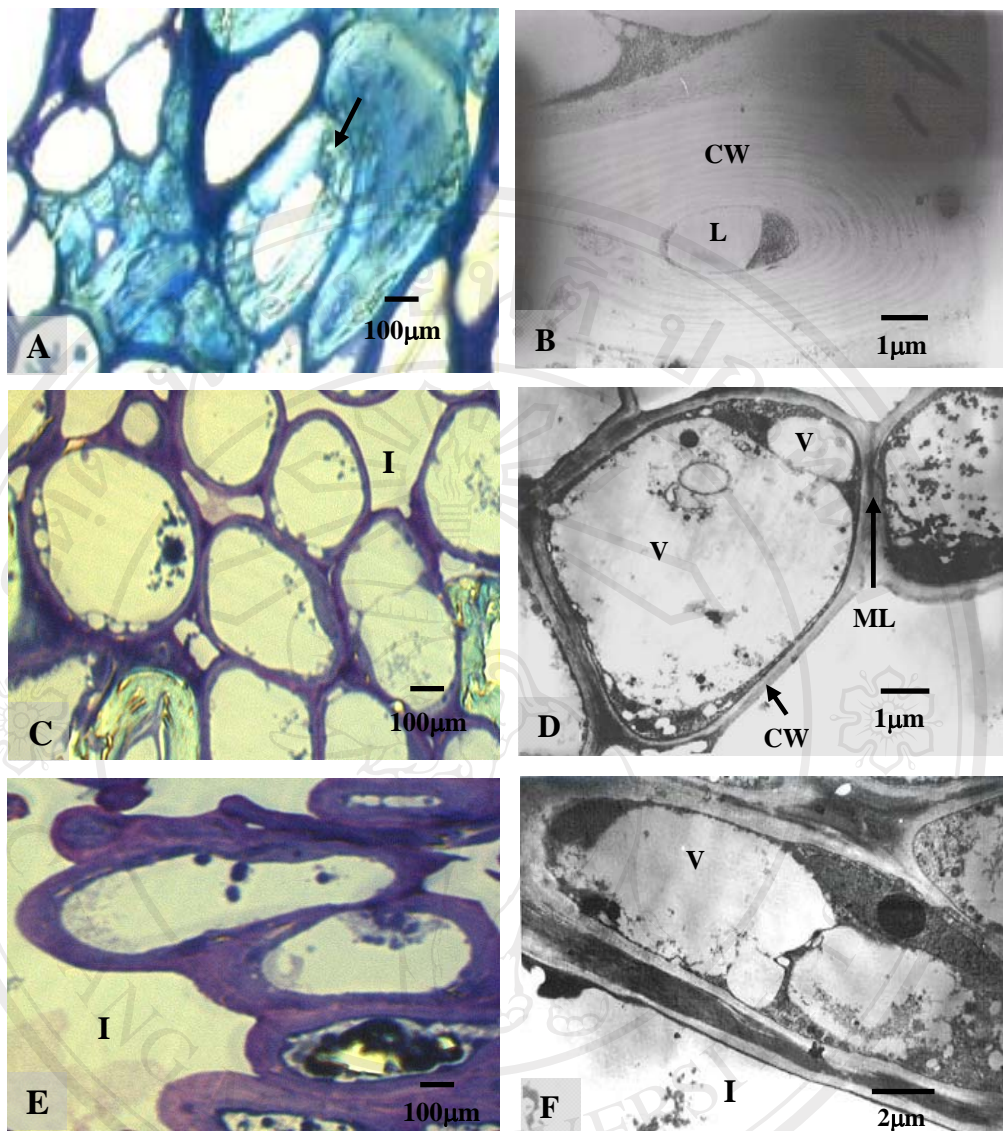


Figure 4.6 LM and TEM micrographs of cells in mesocarp layer.

A = LM micrograph of stone cells showing various cells shape and size (Mag. $\times 100$)

B = TEM micrograph of stone cell showing thick cell wall (Mag. $\times 6,000$)

C = LM micrograph of round shape cells (Mag. $\times 100$)

D = TEM micrograph of round shape cells contained large vacuole and a number of organelles (Mag. $\times 6,300$)

E = LM micrograph of elliptical shape cell with large intercellular space (Mag. $\times 100$)

F = TEM micrograph of elliptical shape cell contained large vacuole with a number of organelles (Mag. $\times 4,000$)

CW = cell wall, L = lumen, ML = middle lamella, V = vacuole

I = intercellular space

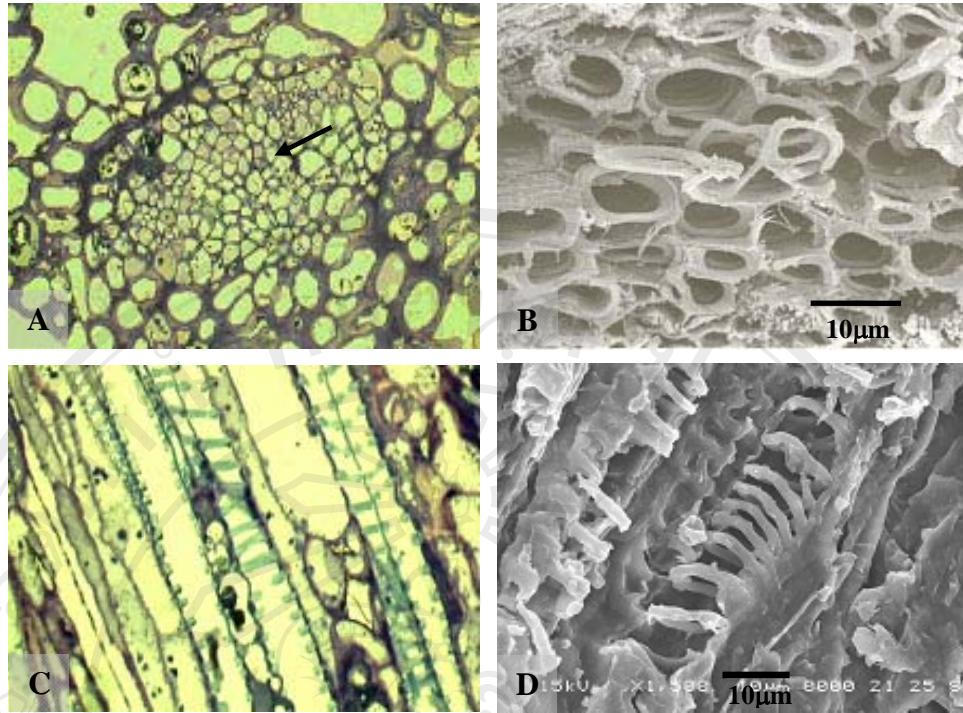


Figure 4.7 LM and SEM micrographs of vascular tissue.

A = Transverse section of vascular tissue (Mag. $\times 40$)

B = SEM micrograph of a group of spirally thickened xylem vessels (Mag. $\times 2,000$)

C = Long section micrograph of xylem vessels (Mag. $\times 40$)

D = SEM micrograph of helical xylem vessels (Mag. $\times 1,500$)

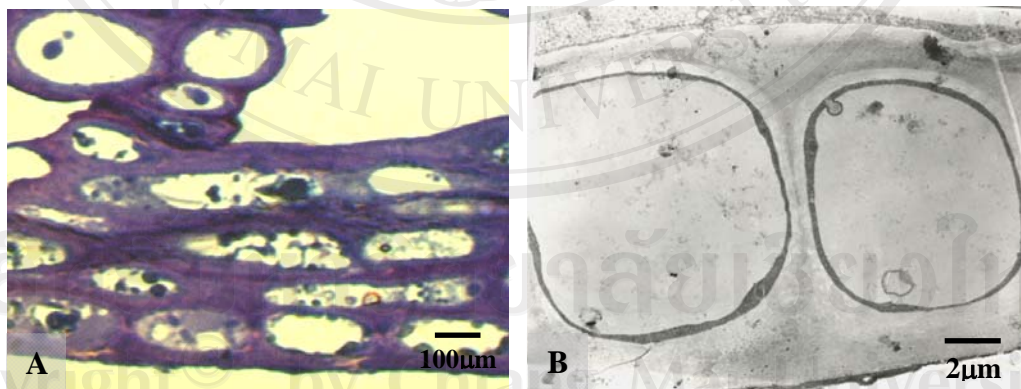


Figure 4.8 LM and TEM micrographs of endocarp layer.

A = LM micrograph of endocarp layer was made up of a square shaped cells in a single layer thick cell walls (Mag. $\times 100$)

B = TEM micrograph of a square shape cell of endocarp with large vacuole and no organelles were evident in these cells (Mag. $\times 4,000$)

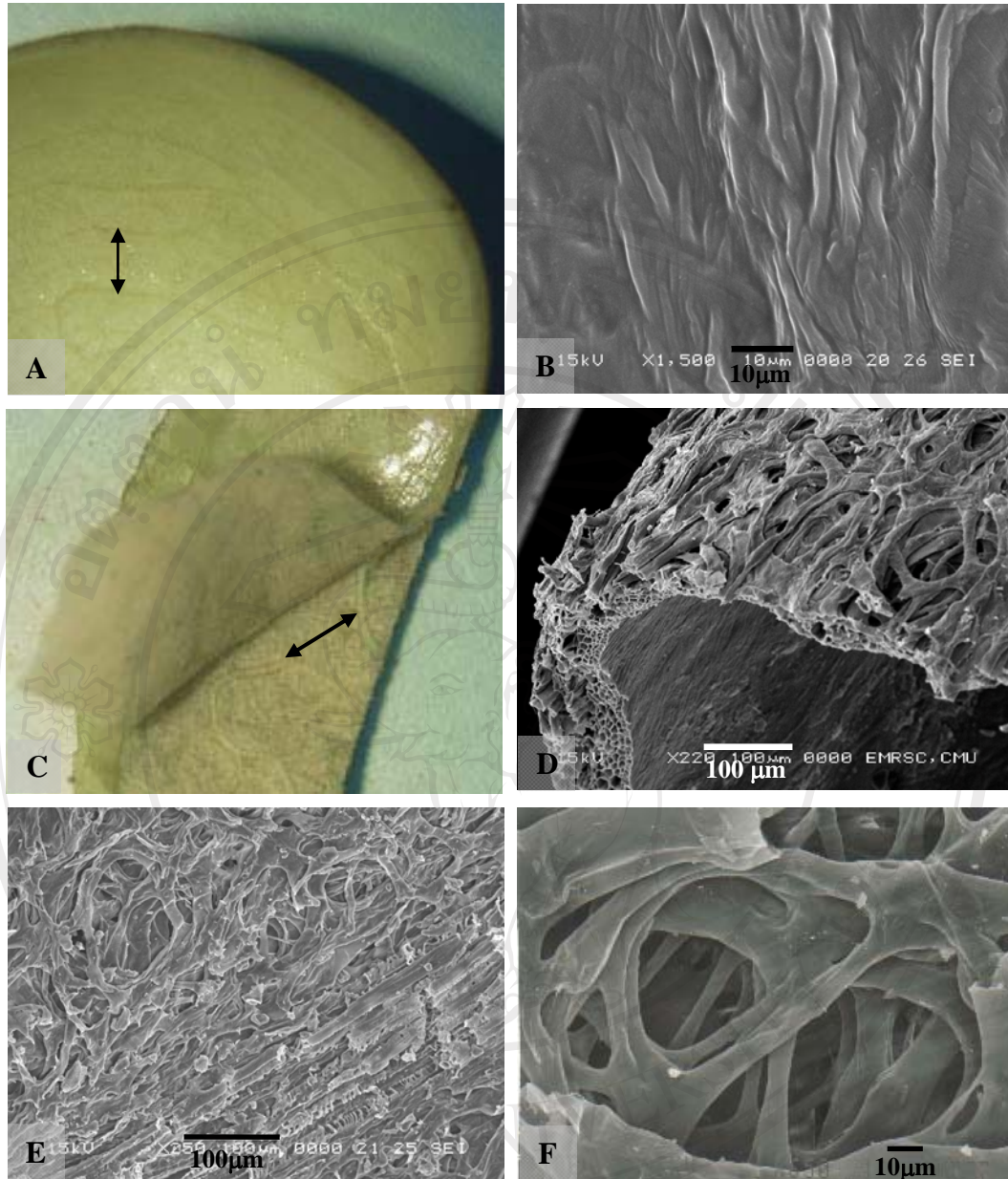


Figure 4.9 The inner surface of longan pericarp cv. Daw.

A = Stereomicrograph of inner surface pericarp showed the waxy with creamy white color (Mag. $\times 4$)

B = SEM micrograph of inner surface pericarp showed light wave on the surface (Mag. $\times 1,500$)

C = Stereomicrograph of longan pericarp when the waxy with creamy white part was peeled, it showed very clear vascular strand (Mag. $\times 4$)

D, E and F = SEM micrographs of a network of connecting tubes in longan pericarp

\longleftrightarrow = Vascular strands on the inner surface pericarp

4.1.2 The anatomy of chilling injured longan fruit pericarp

4.1.2.1 Visual observation of chilling injured longan fruit pericarp

Chilling injury in longan fruit was induced after 6 days of storage at 5°C. Both varieties demonstrated similar chilling injury symptoms. The early stages of chilling injury appeared water-soaked areas and browning of vascular strands of inner surface pericarp. Additionally, the chilling injury manifested as complete browning after 14 days of storage at 5°C. The fruit showed > 2/3 water soaking and browning over the whole fruit after 10 and 14 days of storage in cv. Biew Kiew and Daw, respectively (**Figures 4.10 A-B**). Longan fruit cv. Daw was less sensitive to chilling than cv. Biew Kiew. Severe chilling injury was followed by accelerated susceptibility to decay. The time temperature condition for the development of chilling injury varied with the cultivar and its ecological origin (Wang, 1990). No visible symptoms occurred if stored the fruit at 10°C but the fruit deteriorated more rapidly if stored at 1°C. The symptoms became extremely severe when the fruits were stored at 1°C (Boonyakiat *et al.*, 2002).

4.1.2.2 Stereomicroscope observation of chilling injured longan fruit pericarp

When the chilling injured longan fruit pericarp was viewed under stereomicroscope, browning areas were observed on the outer and inner sides of the pericarp. The inner pericarp exhibited water-soaking (**Figures 4.10 C-D**) and the vascular tissue in the pericarp also showed browning symptom. The most common symptom was a brown strip of vascular strands (**Figure 4.10 E**). The mesocarp cells were the first to turn brown, followed by the endocarp, then the discoloration spreads over the whole pericarp and finally appearing as a darkening of the pericarp surface (**Figure 4.10 F**). These results were similar to those reported by Qu *et al.* (2001). The inside of the skin, affected by chilling damage, was covered with brown blotches rather than being shiny white. Chilling injury was not translocated (Eaks and Morris, 1957). Localized regions of injury could indicate distinct regions of tissue that were more susceptible than the surrounding tissue to chilling temperatures (Wang, 1990).

4.1.2.3 Microscopic anatomy and ultrastructure of chilling injured longan fruit pericarp

The SEM observation showed a layer of injured cells in the pericarp. It was found that the natural cracking, discontinuous cuticle that covered the pericarp and trichomes were damaged in chilling injured pericarp (Figure 4.11). These results agreed with the anatomical changes in lychee pericarp during storage. Underhill and Critchley (1993) found that lychee pericarp browning was correlated with moisture loss. It is very likely that the natural cracking of longan pericarp facilitates rapid moisture loss and caused surface browning after harvest and during storage at ambient temperature. The surface cracking of longan pericarp also helps the chilled air to penetrate through the pericarp during low temperature storage. These can impair the physiological function of the cuticle and increase water permeability (Medeira *et al.*, 1999).

Transverse sectional micrographs of longan pericarp cv. Daw and Biew Kiew were damaged and had microcollapsed of cells especially in mesocarp and endocarp layers (Figure 4.12). The cells and tissues in the mesocarp, including the upper part, middle part and lower part of pericarp were collapsed and also damaged (**Figure 4.13**). The individual upper epidermis on exocarp, the oval shape and elliptical shape cells in the mesocarp exhibited damaged of cell walls (**Figure 4.14**).

The LM observation revealed the damage to the mesocarp cells. The chilling injured cell had undergone separation and dissolution of the middle lamella, as evidenced by the lack of stain between the cells (**Figure 4.15**). The cell ultrastructure of mesocarp cells appeared degradation of cell membranes and deformation of cell walls (**Figure 4.16 B**). The single layer cell in the endocarp showed separation of the middle lamella and damaged of cell membranes (**Figure 4.16 D**). Luza *et al.* (1992) reported that early symptoms of chilling injury were evident in mesocarp cells.

The plasma membrane, although still adjacent to the cell wall, lost wall cohesion and developed an irregular contour. The cytoplasm together with the plasma membrane was pulled away from the cell wall. Changes in the structure of the cell wall appeared during abusive temperature storage. Dissolution of the middle lamella became apparent in some cells as electron-translucent regions and an increasing

fibrillar appearance in the wall. The cell wall underwent separation, beginning at the intercellular spaces and moved along the adjacent cell walls. These physiological disorders might be indicative of subtle damages to the membrane systems (Cutting and Wolstenholme, 1992). Membrane dysfunction might result in increasing permeability to water, apart from a possible effect on loss of subcellular compartmentalization. This would allow enzymes and substrates, sequestered in separate locations, to intermix and initiate browning reactions such as those catalysed by PPO (Vamos-Vigyazo, 1981; Weller *et al.*, 1997).

The injured cells also would accelerate the oxidation of phenolic substances and the oxidative products resulted in dark brown color of inner and outer longan pericarps. The possible occurrence of membrane dysfunction was manifested by an early appearance of skin browning for fruit kept continuously at 5°C. It appeared to precede any discernible structural changes that occurred in the cell wall involving the pectin fraction (Ali *et al.*, 2004). The affected cells showed the larger primary walls to be separated, forming a continuous extracellular matrix. Therefore, some of the major structural changes related to softening and later to chilling injury. Those are related to loosening of cell walls, loss of wall cohesion (Luza *et al.*, 1992).

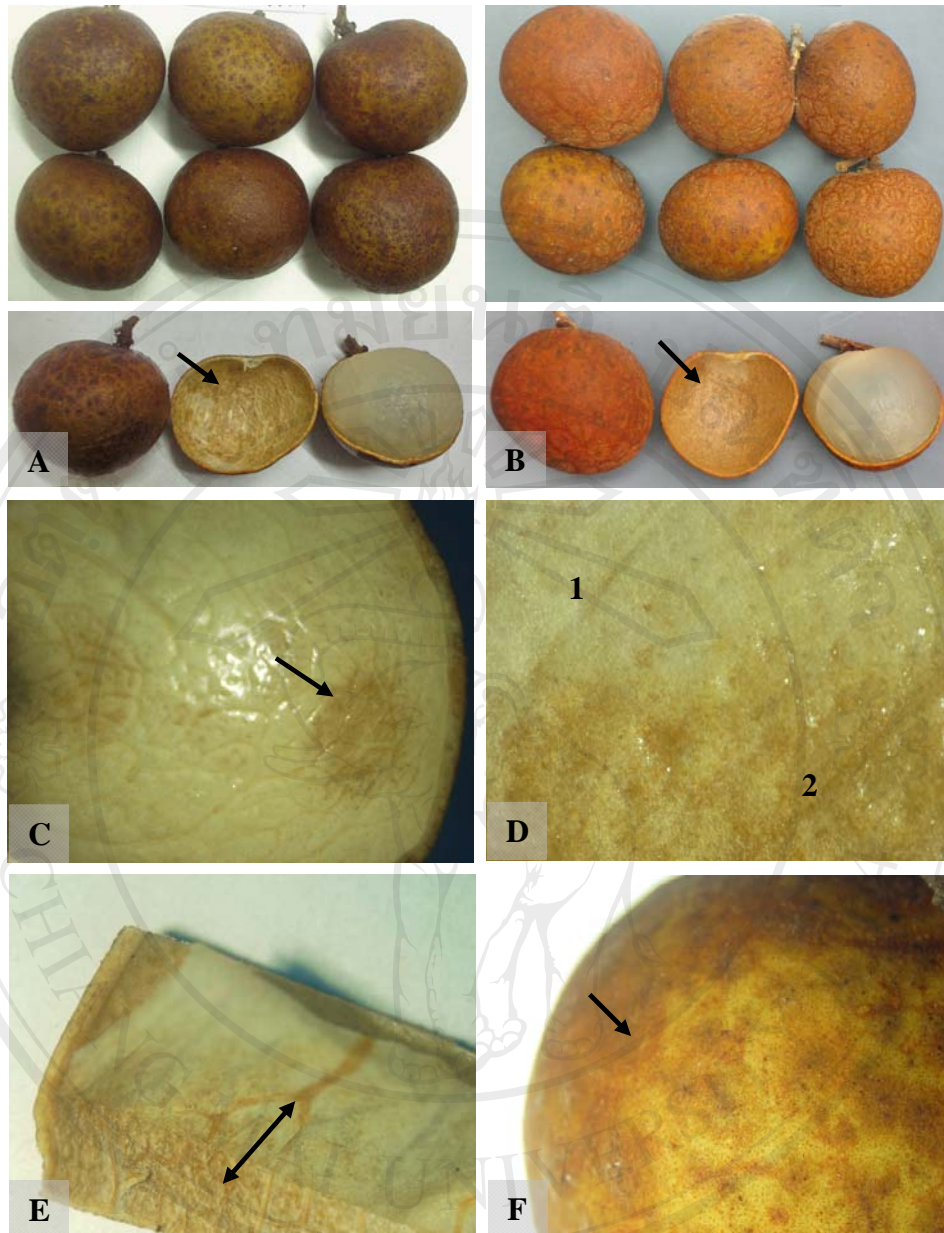


Figure 4.10 Stereomicrographs of chilling injury symptoms of longan fruit pericarps cv. Biew Kiew and Daw during storage for 10 and 14 days at 5°C score 4 showed water soaking and browning >2/3 of outer and inner pericarps.

A = Longan cv. Biew Kiew stored at 5°C for 10 days

B = Longan cv. Daw stored at 5°C for 14 days

C,D = Score 2 of chilling injury showed water soaking and browning spots scattered on the inner surface of pericarp

E = A brown strip of chilling injured vascular strands

F = Discoloration spread over the whole pericarp

1 = Healthy tissue, 2 = Water soaking and browning tissue

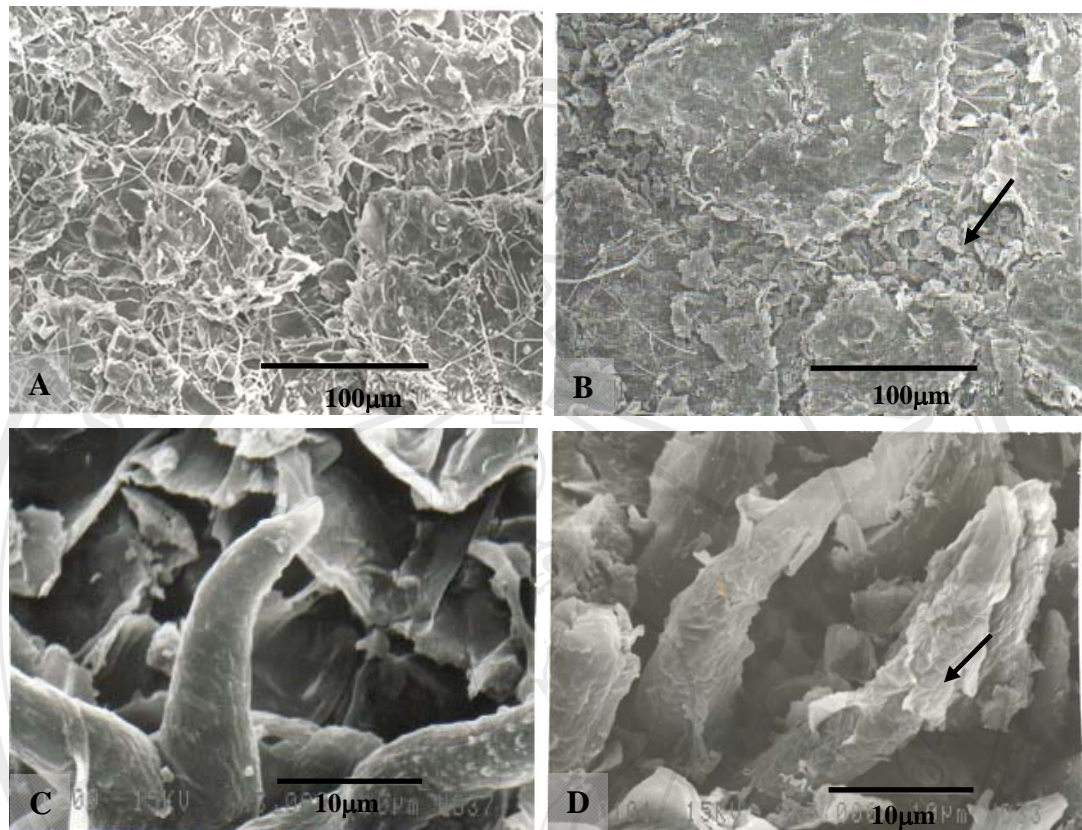


Figure 4.11 SEM micrographs of normal (left) and chilling injured (right) outer pericarp surface of longan fruits.

A = Normal pericarp showed healthy cuticle layer (Mag. $\times 350$).

B = Chilling injured pericarp showed damaged cuticle layer (Mag. $\times 350$).

C = Normal trichomes (Mag. $\times 3,000$)

D = Damaged trichomes on the chilling injured pericarp

Arrows indicate regions of tissue damage

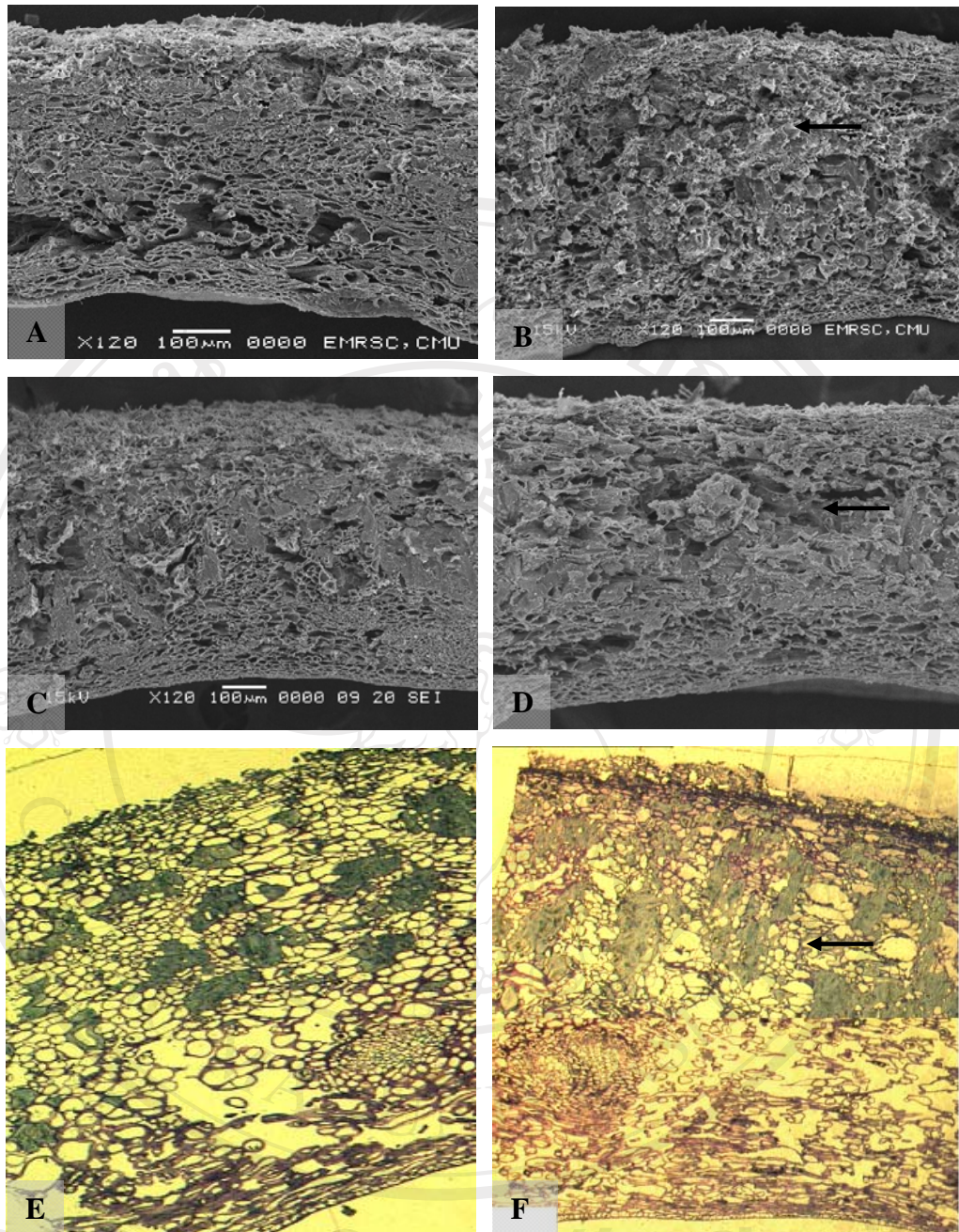


Figure 4.12 Transverse sectional micrographs of normal (left) and chilling injured (right) longan fruit pericarps cv. Daw and Biew Kiew.

A = Normal pericarp cv. Daw (Mag. $\times 120$)

B = Chilling injured pericarp cv. Daw (Mag. $\times 120$)

C = Normal pericarp cv. Biew Kiew (Mag. $\times 120$)

D = Chilling injured pericarp cv. Biew Kiew (Mag. $\times 120$)

E = LM micrograph of normal pericarp cv. Biew Kiew (Mag. $\times 10$)

F = LM micrograph of chilling injured pericarp cv. Biew Kiew (Mag. $\times 10$)

Arrows indicate regions of cell damaged and had collapsed in mesocarp and endocarp layers

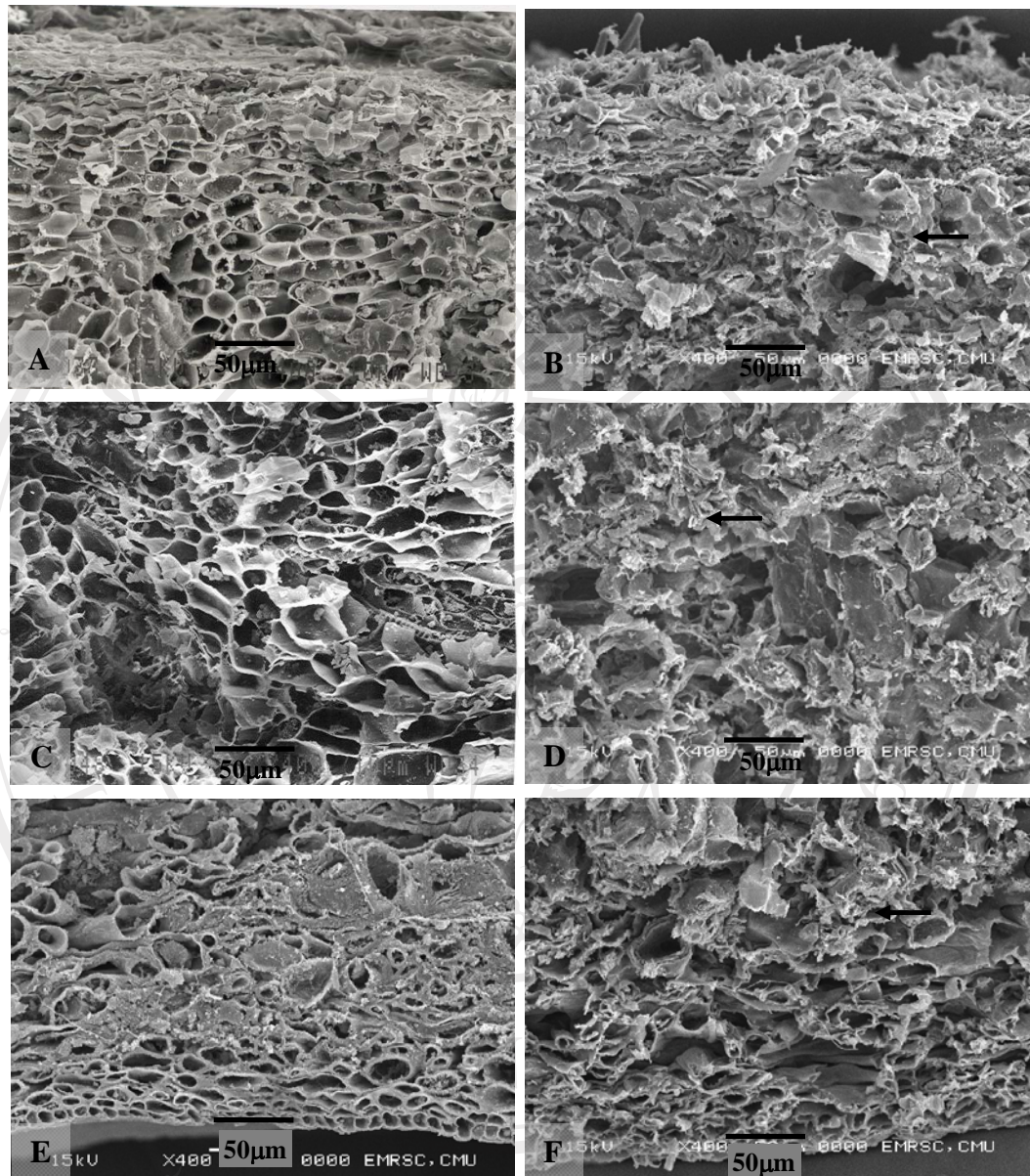


Figure 4.13 Transverse sectional micrographs of normal (left) and chilling injured (right) of longan fruit pericarp cv. Daw.

Arrows indicate regions of cells damaged and collapsed in mesocarp layer

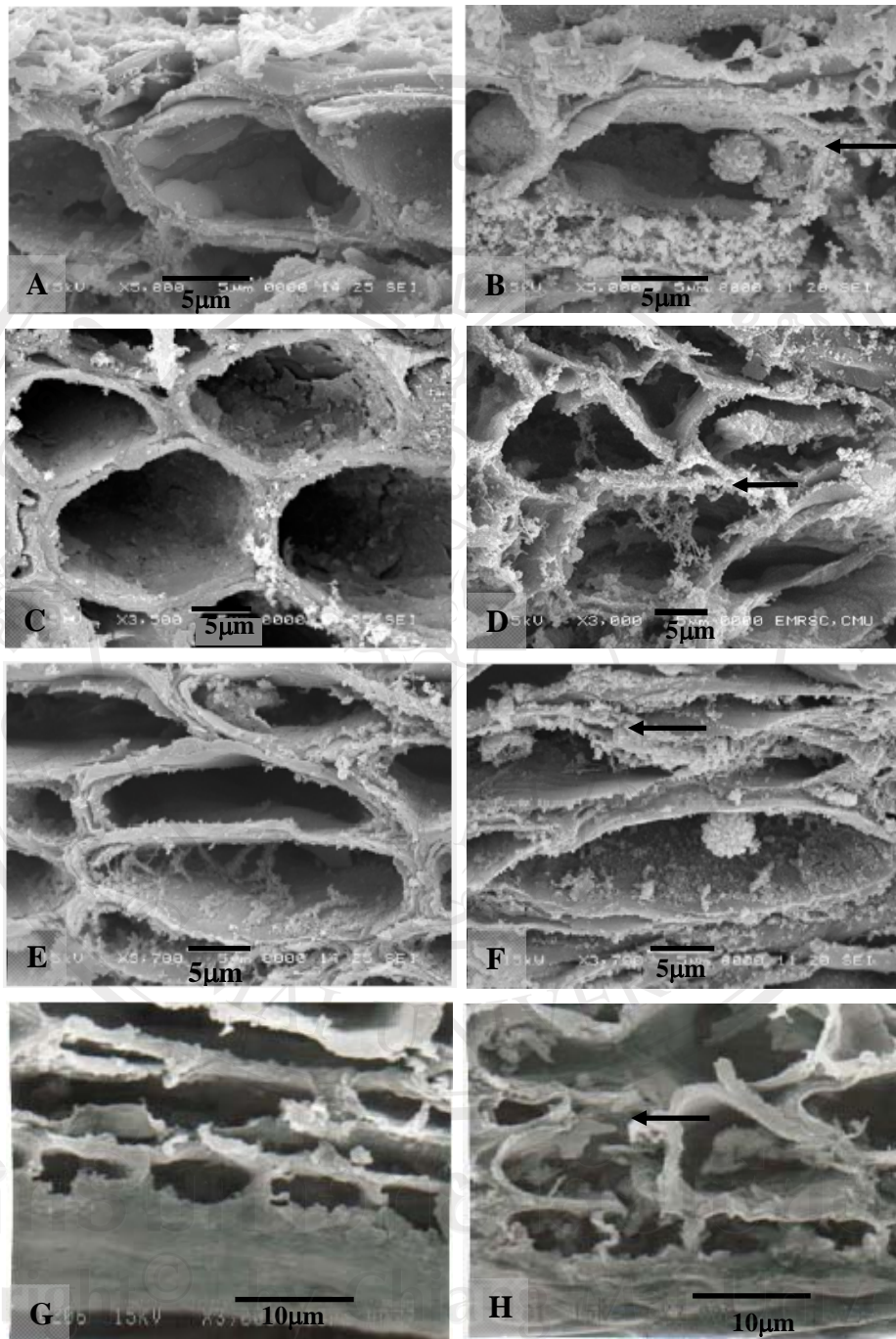


Figure 4.14 Transverse sectional micrographs of normal (left) and chilling injured (right) longan fruit pericarp when viewed with SEM. Arrows indicate of plasma membrane and cell walls damaged and collapsed in mesocarp and endocarp layers

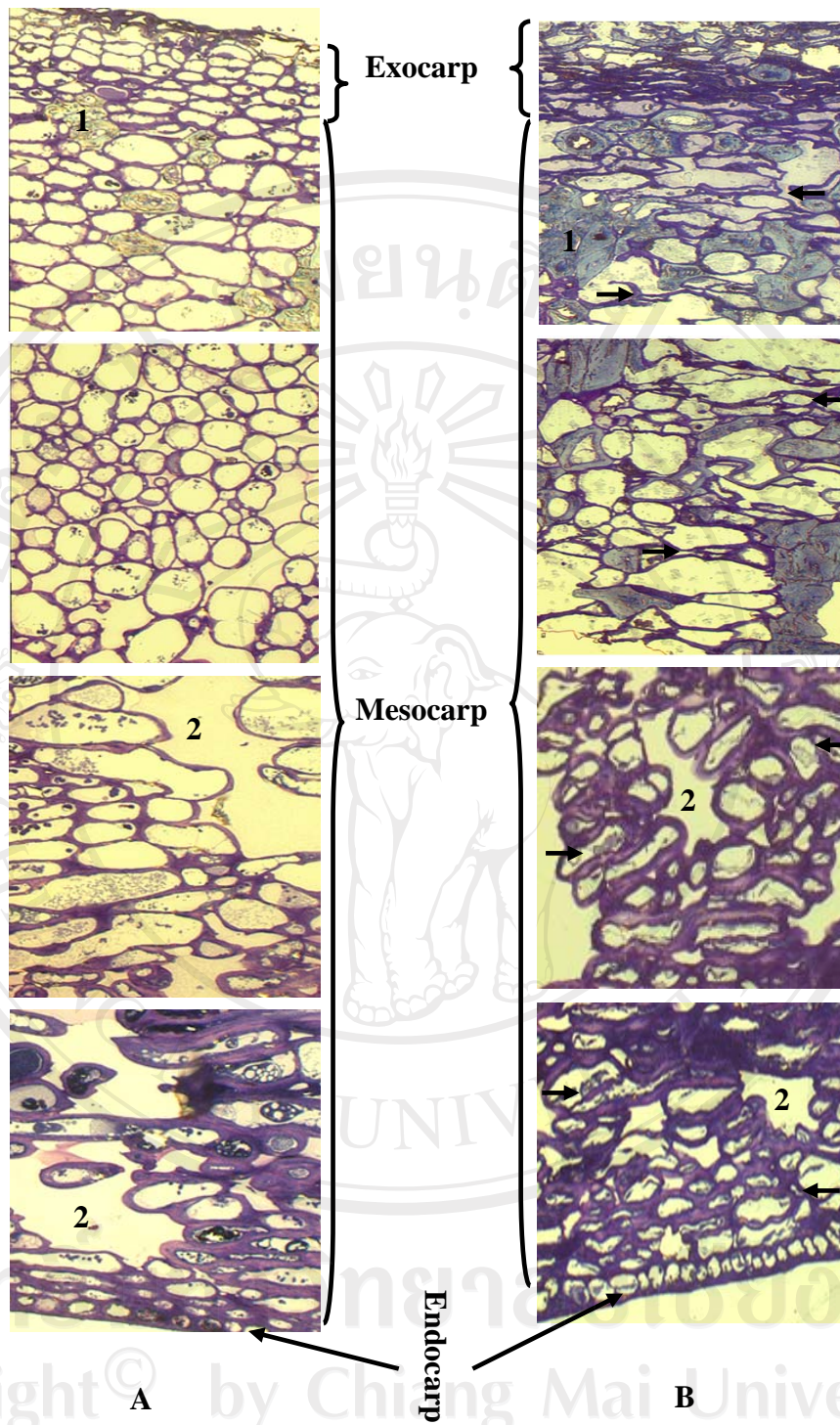


Figure 4.15 Transverse sectional micrographs of normal (left) and chilling injured (right) longan fruit pericarp when viewed with LM.

1 = stone cell, 2 = large intercellular space

Arrows indicate of degradation of cell membranes and deformation of cell walls

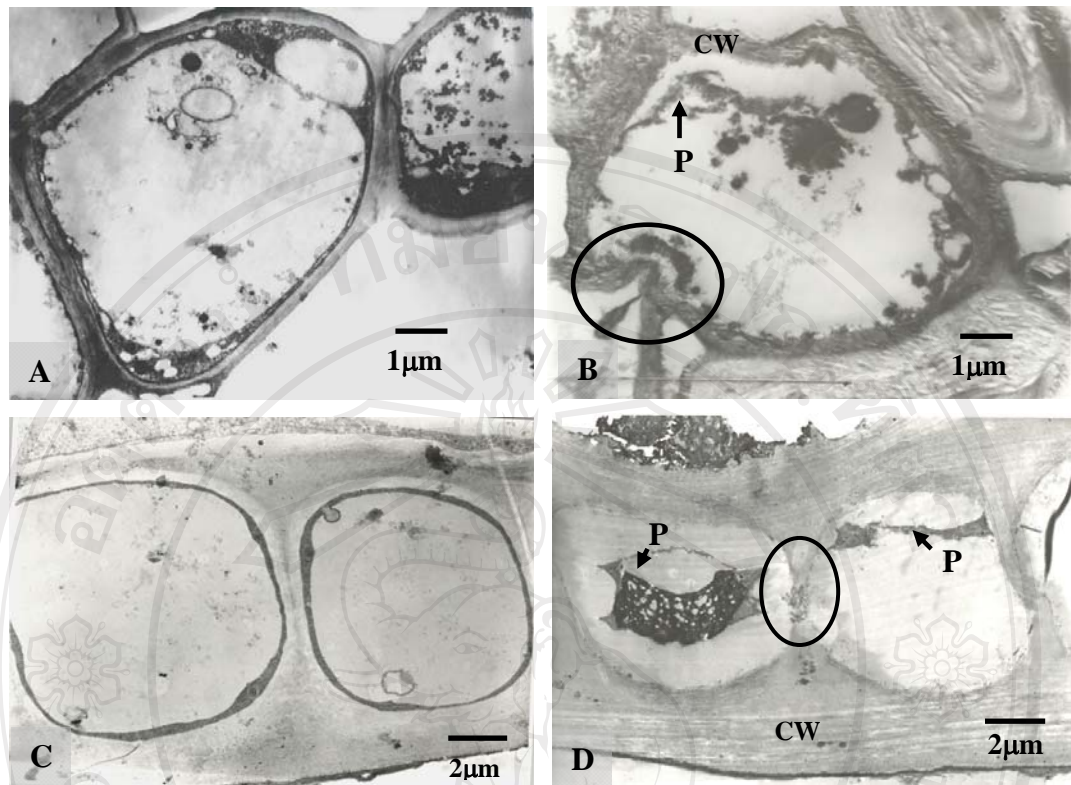


Figure 4.16 TEM micrographs of normal and chilling injured longan fruit pericarp.

A = Normal round shape cell contained intact plasmalemma tightly appressed to the walls (Mag. $\times 6,300$)

B = Chilling injured of round shape cell showed deformation of the cell wall (Mag. $\times 6,300$)

C = Normal single layer of endocarp (Mag. $\times 4,000$)

D = Chilling injured of endocarp showed the plasma membrane became drawn away from the wall (Mag. $\times 4,000$)

CW = cell wall, P = plasma membrane

4.2 Other morphology and anatomy observations of longan fruit

4.2.1 Morphology and anatomy of longan aril

The visual observation of longan arils (flesh) appeared translucent with opaque white color in cv. Daw (**Figure 4.17 A**) and white color in cv. Biew Kiew (**Figure 4.17 B**). The aril tastes sweet in cv. Daw and sharply sweet with crispy in cv. Biew Kiew. The longan arils were observed using SEM (**Figures 4.17 C-D**) and LM (**Figures 4.17 E-F**). It was viewed that the aril composes of parenchymatous tissue with very thin-walled, polyhedral shape cells of various diameters, with large vacuoles and small intercellular space. The aril of chilling injured fruit maintains good quality and still be acceptable. The main sugars present in longan fruit are sucrose, fructose and glucose (Puall and Chen, 1987; Li and Li, 1999). These sugars were stored in parenchyma cells and dissolved in the vacuolar sap (Bowes, 1997). High sugar content in the aril may accelerate fungus infection and fruit decay.

4.2.2 The porosity of longan fruit

An experiment was conducted to test porosity of longan fruit under hypobaric condition. The fruits were immersed under distilled water in a beaker and placed in a vacuum desiccator at 600 mmHg for 2 minutes. Results showed that the longan fruit pericarp has numerous of pores indicated by air bubbles on the surface of fruit under low pressure (**Figure 4.18**). These pores allow passage of water vapor, oxygen and carbon dioxide gas in-and-out of the fruit as well as the chilled air to penetrate through the pericarp during low temperature storage. Both natural cracking and numerous pores on the pericarp can cause longan fruit rapidly lost moisture once harvested.

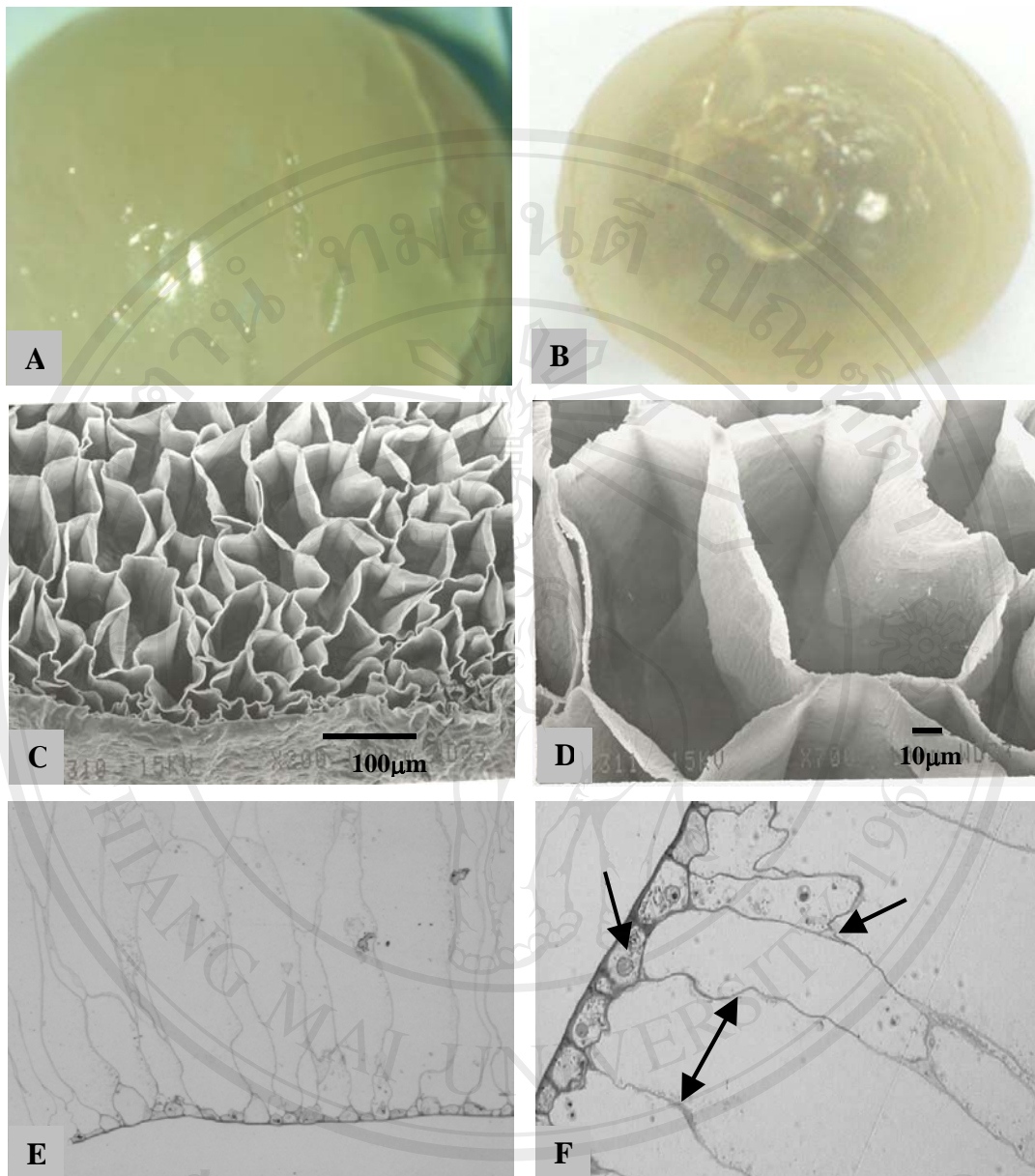


Figure 4.17 Longan aril micrographs of longan cv. Daw and Biew Kiew.

A = Whole longan aril cv. Daw (Mag. $\times 4$).

B = Whole longan aril cv. Biew Kiew (Mag. $\times 4$)

C = SEM micrograph of longan aril was composed of parenchymatous tissue with very thin-walled (Mag. $\times 200$)

D = Polyhedral shape cells with large vacuole and small intercellular space

E = LM micrographs of longan aril by free hand section (Mag. $\times 10$)

F = LM micrographs of longan aril (Mag. $\times 20$)

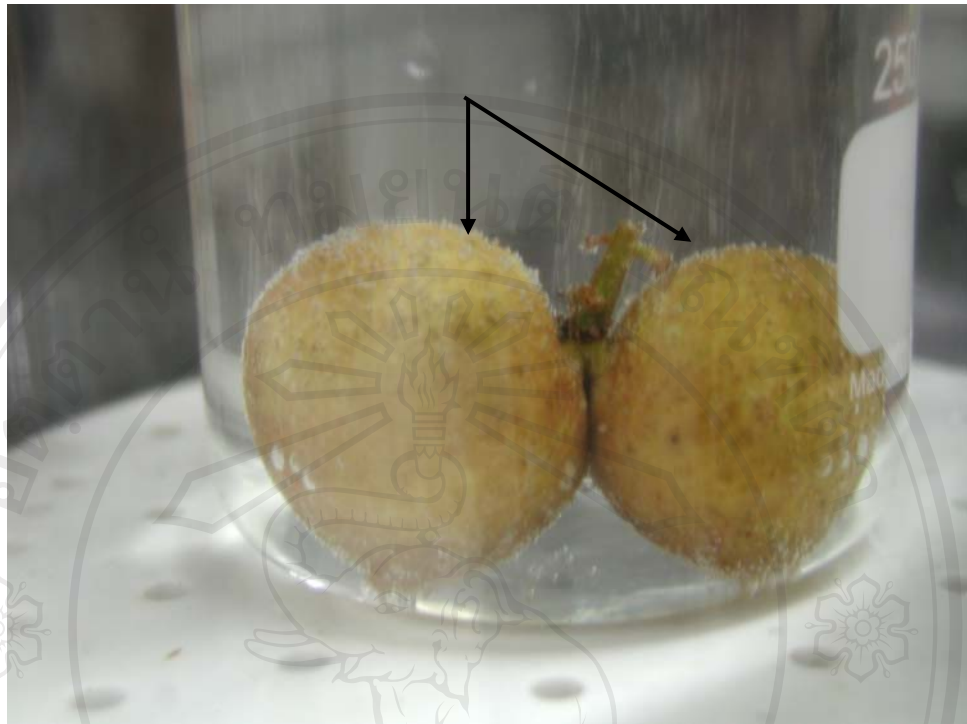


Figure 4.18 The longan fruit pericarp has numerous pores indicating by air bubbles on the surface of fruit under low pressure (hypobaric condition).

Arrows = air bubbles on the surface of fruits.

4.3 Physico-chemical changes between normal and chilling injured longan fruit pericarps

The chilling injury symptoms were mostly apparent in the pericarp. It was indicated by discoloration including water soaking and browning of the inner side of pericarp. The symptoms steadily increased and dispersed to both sides of the pericarp causing the whole fruit to become brown within 10 and 14 days of storage at 5°C for cv. Biew Kiew and Daw, respectively. **Tables 4.1-4.4** showed the physico-chemical changes of longan pericarp such as increased degree of browning and decreased L^* values, changes in electrolyte leakage and moisture content. The severe symptom was the development of water-soaked tissue and became deterioration and decay. Paull and Chen (1987) reported that chilling injury symptoms can be reduced by modified atmosphere storage in polyethylene bags up to 5 weeks at 1°C. However, the pericarp appeared dark brown and dried during storage, with little changes in composition and flavor.

4.3.1 Measurement of the pericarp color

The L^* values of longan fruit pericarps cv. Daw and Biew Kiew during storage at 5°C decreased from 53.20 to 41.62 and 43.66 to 34.69 for the outer side and decreased from 82.46 to 67.29 and 81.65 to 75.36 for the inner side, respectively (**Tables 4.1** and **4.2**). Rattanapanone *et al.* (2001) reported that L^* values of outer side of longan fruit pericarp cv. Daw decreased from 52.41 to 46.92 and those of inner side decreased from 76.98 to 64.75 during storage at 5°C for 14 days. The L^* values of cv. Biew Kiew decreased faster than cv. Daw with not significant difference ($P>0.05$). The development of browning and severity of chilling injury was characterized by decreasing in L^* values.

4.3.2 Determination of moisture content of pericarp

The moisture content of longan fruit pericarp cv. Daw and Biew Kiew decreased 47 and 22% of the initial values during storage at 5°C for 14 and 10 days, respectively (**Table 4.3**). These results showed that the pericarp from longan cv.

Daw exhibited higher moisture loss than cv. Biew Kiew. Chilling injury symptoms were closely related with damaged of cuticle layer and also trichomes on the pericarp surface, perhaps causing increased loss of moisture content and effecting to browning potential as reflected by increased PPO activities (**Table 4.5**). The moisture loss increased during chilling injury is probably due to cracking, porosity and cell wall damage on the pericarp.

4.3.3 Determination of electrolyte leakage

Symptoms of chilling injury of fruit associated with the changes in membrane permeability. Membrane permeability is an expression of the freedom with which water and solutes can pass through the membrane. Increased permeability of membranes may be limited to special cells in the parenchymal tissues and may cause the promotion of an enzyme-substrate interaction, resulting in the occurrence of scald, discoloration, browning and an increase in respiratory rate. Changes in membrane permeability of phenol substances may be the cause of browning tissues. Permeability can be assessed by the measurement of the rate of leakage of solutes, including ions from the tissues. Membrane permeability also depends upon ripening and senescence of fruit tissues (Wang, 1990).

The electrolyte leakage of pericarp disks from both cultivars during storage at chilling temperature (5°C) was studied. The electrolyte leakage of longan pericarps cv. Daw and Biew Kiew after storage for 14 and 10 days increased from 12.61 to 47.52% and from 8.89 to 23%, respectively (**Table 4.4**). Electrolyte leakage of longan fruit cv. Daw during storage at 5°C for 14 days increased from 9.85 to 52.50% and step-wise temperature conditioning decreased electrolyte leakage (Rattanapanone *et al.*, 2001).

Table 4.1 L* values of outer pericarp surfaces cv. Daw and Biew Kiew during storage at 5 and 10°C.

Cultivar	Temperature (°C)	Day of storage*							
		0	2	4	6	8	10	12	14
Daw	5	53.20±1.2 ^a	49.40±1.0 ^a	47.82±0.9 ^a	46.70±0.8 ^b	45.08±1.1 ^b	42.84±0.6 ^b	42.58±0.6	41.62±1.3
	10	53.20±1.2 ^a	49.59±1.0 ^a	49.21±0.8 ^a	48.84±0.7 ^a	47.71±0.9 ^a	45.30±1.1 ^a	44.46±0.9	43.52±1.0
Biew Kiew	5	43.66±0.5 ^b	37.81±0.7 ^c	38.17±0.6 ^b	35.36±0.8 ^c	34.85±0.4 ^c	34.69±0.8 ^c		
	10	43.66±0.5 ^b	40.73±0.8 ^b	38.72±0.8 ^b	36.36±0.8 ^c	35.45±0.5 ^c	35.75±0.7 ^c		
LSD _{0.05}		2.65	2.59	2.26	2.68	2.05	2.37		
C.V. (%)		6.68	7.10	6.35	7.84	6.07	7.28		

*Means within the same column followed by different letters are significantly different at 95% ($P \leq 0.05$) level by Least Significant Difference comparison. Data are mean values \pm SE.

Table 4.2 L* values of inner pericarp surfaces cv. Daw and Biew Kiew during storage at 5 and 10°C.

Cultivar	Temperature (°C)	Day of storage*							
		0	2	4	6	8	10	12	14
Daw	5	82.46±0.9 ^a	77.20±0.9	69.81±1.7 ^b	75.85±0.6 ^b	73.17±0.9 ^c	69.96±1.3 ^c	67.34±0.7	67.29±0.5
	10	82.46±0.9 ^a	77.08±0.9 ^b	79.37±0.4 ^a	75.39±0.8 ^b	79.04±0.5 ^b	74.89±0.3 ^b	73.34±0.7	70.84±0.8
Biew Kiew	5	81.65±0.5 ^a	81.59±0.3 ^a	79.65±0.4 ^a	79.47±0.5 ^a	78.41±0.5 ^{ab}	75.36±1.3 ^b		
	10	81.65±0.5 ^a	80.00±0.6 ^a	81.00±0.5 ^a	80.25±0.4 ^a	80.29±0.2 ^a	79.48±0.6 ^a		
LSD _{0.05}		2.33	2.15	2.80	1.78	1.76	2.93		
C.V. (%)		3.47	3.31	4.40	2.79	2.74	4.77		

*Means within the same column followed by different letters are significantly different at 95% ($P \leq 0.05$) level by Least Significant Difference comparison. Data are mean values \pm SE.

Table 4.3 Moisture content of longan pericarps cv. Daw and Biew Kiew during storage at 5 and 10°C.

Cultivar	Temperature (°C)	Day of storage*							
		0	2	4	6	8	10	12	14
Daw	5	59.47±0.2 ^a	51.87±0.3 ^b	49.23±0.4 ^b	44.00±1.2 ^c	44.47±2.8 ^b	43.31±0.7 ^b	37.26±1.9	31.96±1.5
	10	59.47±0.2 ^a	52.42±0.4 ^{ab}	48.55±3.1 ^b	48.95±0.7 ^b	42.28±2.6 ^c	43.93±0.9 ^b	35.11±0.7	32.41±2.8
Biew Kiew	5	57.87±0.2 ^b	54.13±0.9 ^a	53.50±0.8 ^a	52.18±0.4 ^a	48.95±0.6 ^a	46.51±0.7 ^a		
	10	57.87±0.2 ^b	53.49±0.9 ^{ab}	52.00±0.5 ^a	52.92±1.3 ^a	48.53±0.9 ^a	45.43±0.8 ^{ab}		
LSD _{0.05}		0.85	2.09	1.65	2.87	2.23	2.40		
C.V. (%)		1.35	3.59	4.57	5.26	3.80	4.86		

*Means within the same column followed by different letters are significantly different at 95% ($P \leq 0.05$) level by Least Significant Difference comparison. Data are mean values \pm SE.

Table 4.4 Electrolyte leakage of longan pericarps cv. Daw and Biew Kiew during storage at 5 and 10°C.

Cultivar	Temperature (°C)	Day of storage*							
		0	2	4	6	8	10	12	14
Daw	5	12.61±0.4 ^a	18.40±0.2 ^a	23.44±0.7 ^a	29.83±1.6 ^a	29.17±1.3 ^a	29.86±0.6 ^a	39.11±1.1	47.52±0.6
	10	12.61±0.4 ^a	16.12±0.7 ^b	17.13±0.8 ^b	22.54±0.2 ^b	22.85±1.0 ^b	23.30±1.1 ^b	32.49±1.9	34.82±1.1
Biew Kiew	5	8.66±0.6 ^b	13.70±0.1 ^c	18.30±0.9 ^b	17.30±0.4 ^c	20.85±0.3 ^{bc}	24.73±1.3 ^b		
	10	8.66±0.6 ^b	12.28±0.1 ^d	16.64±0.4 ^b	17.45±1.0 ^c	19.55±0.1 ^c	22.31±1.6 ^b		
LSD _{0.05}		1.08	1.15	1.82	3.16	2.58	3.67		
C.V. (%)		8.46	6.31	7.45	12.84	9.28	11.06		

*Means within the same column followed by different letters are significantly different at 95% ($P \leq 0.05$) level by Least Significant Difference comparison. Data are mean values \pm SE.

Copyright © by Chiang Mai University
All rights reserved



ลิขสิทธิ์มหาวิทยาลัยเชียงใหม่

Copyright© by Chiang Mai University

All rights reserved

4.4 The relationships between polyphenol oxidase activity and electrolyte leakage of longan pericarp during chilling injury of longan fruit cv. Daw

The relationships between biochemical changes and chilling injury ratings of longan pericarp were studied only in cv. Daw during storage at 5°C. For analysis of PPO activity, the whole pericarp was separated into 2 parts, the inner pericarp (endocarp and lower mesocarp include some parts of vascular tissues, 100 µm thick) and outer pericarp (mid-upper mesocarp and endocarp, 400 µm thick) (**Figure 4.19**). The visible signs of chilling injury was initiated with clearly changes in the inner pericarp after storage for 8 days. Additionally, electrolyte leakage of longan pericarp increased and PPO activity of the inner pericarp sharply increased while L* value gradually decreased (**Table 4.5**). Following, the electrolyte leakage of outer pericarp gradually increased, PPO activity increased and then gradually decreased until the discoloration spread over the whole pericarp and complete darkening after 14 days storage.

The PPO activity of inner pericarp increased first with showed peak on day 10, following the outer pericarp PPO activity showed peak on day 12. These results can explain the positive relationship between PPO activity, electrolyte leakage and chilling injury development of longan pericarp. These results demonstrated the correlation between pericarp structure, damaged cell membranes (loss of membrane permeability), damaged cell wall, collapsed of cells in mesocarp and PPO activity with chilling injury development.

The loss of subcellular compartmentalization allows PPO, which localized in the plastids to act on the phenolic compounds as PPO substrates, which localized in vacuole due to leakage of cell membranes and initiate enzymatic browning reactions and developed brown-colored byproducts (Lee and whitaker, 1995). Finally the natural opening of longan pericarp facilitates rapid moisture loss and cause surface browning after harvest and during storage. The damaged surface of longan pericarp also helps the chilled air to penetrate through the pericarp during low temperature storage. The damaged cuticle and trichomes could be enhanced by dehydration while a water deficit was an essential prerequisite for CI induced solute leakage.

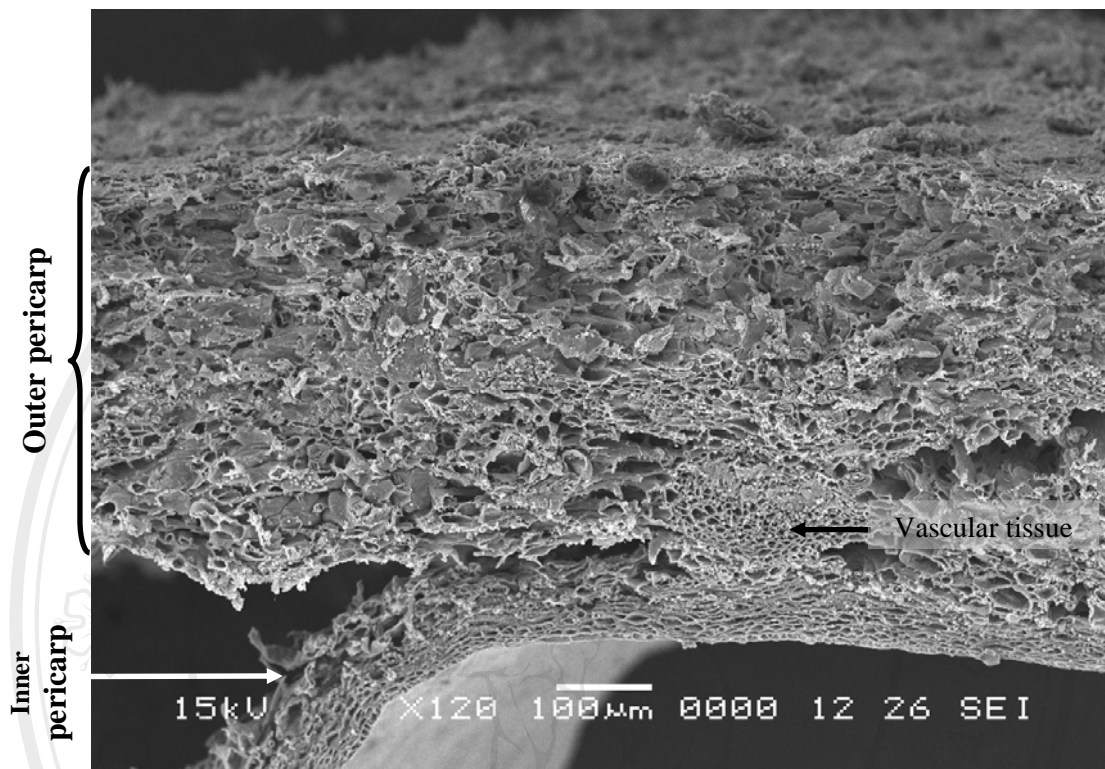


Figure 4.19 The pericarp was separated into 2 parts of whole pericarp for activity analysis showed the inner pericarp (endocarp and lower mesocarp include some parts of vascular tissue) and outer pericarp (mid-upper mesocarp and endocarp) when viewed with SEM.

Table 4.5 The L* values, PPO activity and electrolyte leakage of longan fruit pericarp cv. Daw during storage at 5°C for 14 days.

Parameter	Day of storage								LSD _{0.05}	C.V. (%)
	0	2	4	6	8	10	12	14		
L* outer ¹	50.54±0.4 ^a	45.19±2.1 ^b	41.42±1.5 ^c	41.01±1.2 ^c	40.80±3.0 ^c	38.68±1.9 ^d	38.32±2.0 ^d	38.07±1.8 ^d	1.11	4.68
L* inner ²	83.73±1.8 ^a	81.17±1.5 ^b	79.36±2.1 ^c	78.25±2.0 ^c	77.55±2.3 ^{cd}	74.72±3.5 ^e	72.56±1.8 ^f	71.99±1.5 ^f	1.26	2.89
PPO outer ³	65.78±0.5 ^f	79.61±0.5 ^e	82.54±0.5 ^d	80.86±0.5 ^e	91.95±0.7 ^c	106.43±0.7 ^b	160.21±0.6 ^a	60.78±0.5 ^g	1.61	1.02
PPO inner ⁴	61.66±0.8 ^f	74.10±0.4 ^d	74.29±0.5 ^d	71.65±0.6 ^e	95.43±0.5 ^c	197.77±0.6 ^a	152.28±0.5 ^b	61.45±0.5 ^f	1.69	0.99
EL ⁵	9.95±0.8 ^e	13.37±0.9 ^d	15.17±0.6 ^d	16.05±0.8 ^d	20.45±0.9 ^c	31.55±0.8 ^b	32.00±0.8 ^b	38.91±0.7 ^a	3.27	11.43

¹Outer pericarp surface, ²Inner pericarp surface, ³Outer part of pericarp, ⁴Inner part of pericarp, ⁵Electrolyte leakage.

*Means within the same row followed by different letters are significantly different at 95% ($P \leq 0.05$) level by Least Significant Difference comparison. Data are mean values \pm SE.



ลิขสิทธิ์มหาวิทยาลัยเชียงใหม่

Copyright© by Chiang Mai University

All rights reserved

4.5 To identify the main classes of phenolic compounds and other components of normal and chilling injured longan fruit pericarps

The phenolic compounds in the pericarps of longan fruit (cv. Daw and Biew Kiew) were analyzed using HPLC and LC-MS. The objective of this study was to provide an initial characterization of the main classes and also to identify type of phenolic compounds in normal and chilling injured of longan fruit pericarps. The characterization contributes to the understanding of the biochemical transformations in the pericarp resulting from chilling injury during postharvest storage. Phenolics with different structures are likely to have different chemical and biological properties (Soong and Barlow, 2005).

4.5.1 Number and identification of phenolic compounds in longan fruit pericarps cv. Daw and Biew Kiew

The phenolic compounds in the pericarp of two varieties of longan were analyzed by HPLC-PDA-MS. These analyses were conducted on the pericarp of normal and on chilling injured fruits. These initial analyses appeared a large number of UV-absorbing compounds in the pericarp extracts. The result did not show clearly distinguishable differences between the pericarp of normal and chilling injured fruits of either variety of longan. Part of this failure to detect any clear differences was due to the large number of peak overlaps in the HPLC chromatograms (Figure 4.20). Hence, accurate UV (PDA) and MS analyses of many compounds in the longan pericarp were not possible.

To achieve HPLC peak separations sufficient for accurate UV (PDA) and MS analysis, the phenolic compounds in these extracts were fractionated by Biogel-P2 size-exclusion chromatography. The result showed the resolution of several classes of phenolic compounds, including ellagic acid conjugates, flavonoid glycosides, and other unknown compounds. **Figure 4.21** showed the HPLC chromatograms of three sequential P2 column fractions in which these classes of compounds were detected. The initial-eluting P2 column fractions contained broad, poorly resolved sets of compounds, similar to those previous described in early-eluting size-exclusion LH20

chromatographic fractions of longan seed extracts (Soong and Barlow, 2005). The subsequently eluting P2 column fractions contained ellagic acid conjugates and a specific group of unknown compounds (**Figure 4.21 A-B**). Later eluting fractions contained flavone glycosides (**Figure 4.21 C**). Other compounds in these main classes of phenolic compounds were similarly detected in other fractions.

Figure 4.22 showed the UV and MS of the major ellagic acid conjugates detected in the freeze-dried normal longan pericarp. The compounds were initially identified by their UV spectra, which matched that of an ellagic acid standard. The compounds were further detected by the presence of the mass ion at 303 m/z , which matched the protonated molecular weight $(M+H)^+$ of ellagic acid. The 303 m/z ion was particularly evident at higher cone voltages (fragmentation energies) i.e. 60V, whereas at the lower cone voltage, i.e. 20V, higher mass ions were detected that were consistent with the neutral losses of hexoses (146 amu for possible rhamnose), and a pentose (132 amu). The MS data indicated that the main ellagic acid conjugates in normal longan pericarp are glycosides.

HPLC-PDA-MS analysis of the later-eluting P2 column fractions showed the presence of a number of flavonoid glycosides. Two classes were identified, including quercetin glycosides and kaempferol glycosides. Acid hydrolysis of longan pericarp extracts produced two flavone aglycones, which when analyzed by HPLC-PDA-MS exactly matched the elution times, UV, and MS of authentic samples of quercetin and kaempferol.

The quercetin glycosides were detected by their UV spectra, which were characteristics of numerous previously reported quercetin glycosides (Mabry *et al.*, 1970). The presence of a mass ion of 303 m/z , which matched the protonated molecular weight $(M+H)^+$ of quercetin (**Figure 4.23**). Three of the compounds (**A-C**) exhibited higher mass ions suggesting the neutral losses of hexoses (162 amu of possible glucose [(465 amu-303 amu), in **Figures 4.23 B-C**] and 146 amu for rhamnose [(449 amu-303 amu), in **Figure 4.23 A**]. The two remaining compounds (**D and E**) exhibited two higher mass ions, suggestive of the neutral losses of both a glucose and a rhamnose moiety. An additional compound exhibited fragment ions as indicative of a quercetin trisaccharide (Q + glucose + 2 rhamnose).

The UV and MS spectra of the two main kaempferol glycosides are shown in **Figure 4.24**. Both compounds exhibited UV spectra characteristic of previously reported kaempferol glycosides (Mabry *et al.*, 1970). Mass ion

fragments at 287 m/z , matching the protonated molecular weight $(M+H)^{+1}$ of kaempferol. The MS of compound A demonstrated the neutral loss (419 amu-287 amu) of 132, possibly a pentose, while compound B exhibited the neutral loss (449 amu-287 amu) of 162, matching a hexose, possibly glucose. As shown in Table 4.6, three additional kaempferol glycosides were detected, including a rhamnoside (shown by a neutral loss of a single 146 amu fragment), and 2 disaccharides (both exhibiting neutral losses of 162, and 146, possibly glucose and rhamnose, respectively). In the present study, it can be concluded that the **main classes of phenolic compounds in freeze-dried longan pericarp identified by HPLC-PDA-MS were ellagic acid glycosides, kaempferol glycosides and unknown compounds (Table 4.7).**

The phenolic compounds have been previously reported in longan pericarp, aril and seed. Longan pericarps were extracted with methanol : acetone : water (4.5 : 4.5 : 1) then were separated and purified by polyamine column chromatography, Sephadex LH-20 column chromatography, and silica gel column chromatography. On the basis of 1H NMR, ^{13}C NMR and electrospray ionization mass spectrometric (ESI-MS) data, the two compounds were identified as 4-*O*-methylgallic acid and (-)-epicatechin, respectively (Sun *et al.*, 2007).

Soong and Barlow (2005) identified gallic acid and ellagic acid from longan seeds by reverse-phase (RP) HPLC coupled with photodiode array detection. Rangkadilok *et al.* (2005) studied the polyphenols extracted with 70% methanol from pericarp, aril and seed tissues of longan fruit. The identified major components were gallic acid, corilagin (an ellagitannin), and ellagic acid. These three compounds in different parts of the longan fruit and among different cultivars were large variation in the content. Seed contained the highest levels of the three phenolics and aril contained the lowest. Among cultivars, Biew Kiew and Daw contained the highest level of gallic and ellagic acids while Srichompoo contained the highest content of corilagin.

Fresh and dried arils and seeds of longan fruit contained gallic acid while the pericarp contained gallic acid only in dried tissues. The contents of gallic acid were higher in dried tissues (pericarp and seed) than fresh tissues.

However, fresh aril contained higher levels of gallic acid than dried aril on dry weight basis except for cv. Daw (Rangkadilok, *et al.* (2005).

HPLC-ESI-MS analysis has revealed the phenolics profile of longan seed. There were 14 positively identified phenolic compounds comprising of gallic acid, ellagic acid, monogalloyl-glucose, monogalloyl-diglucose, digalloyl-diglucose, penta- to heptagalloyl-glucose, ellagic acid-pentose conjugate, galloyl-HHDP (hexahydroxydiphenyl)-glucopyranose, pentagalloyl-HHDP-glucopyranose, procyanidin A-type dimer, procyanidin B2 and quercetin-3-O-rhamnoside (Soong and Barlow, 2005, 2006)

Mahattanatawee *et al.* (2006) detected ellagic acid conjugates and flavone glycosides, consisting mainly of quercetin and kaempferol in longan aril.

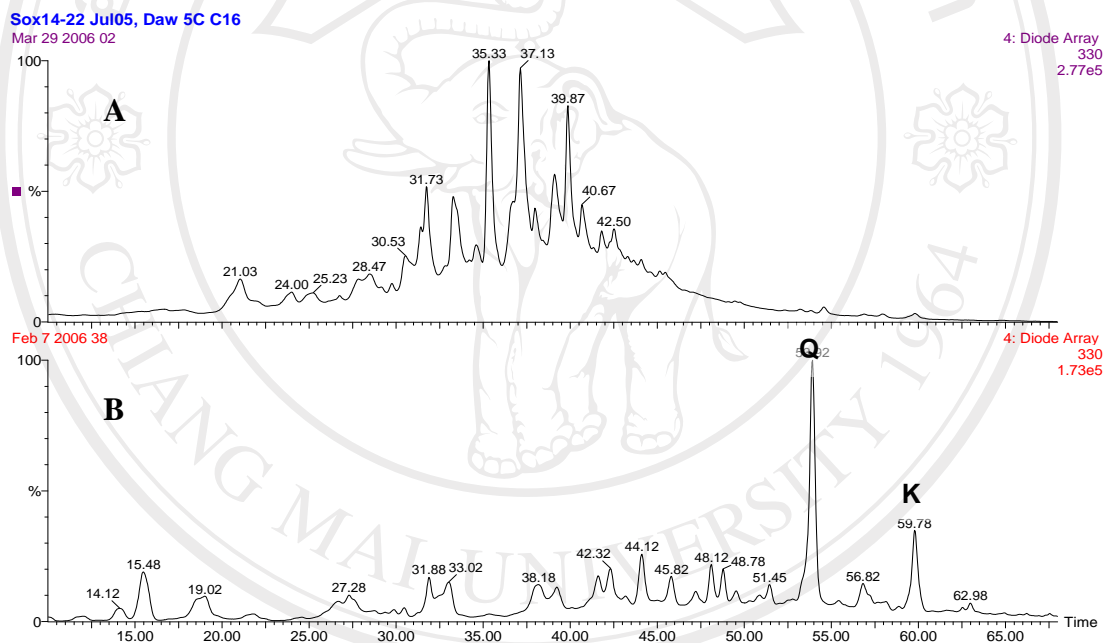


Figure 4.20 The large number of peak overlaps in the HPLC chromatograms showed many of the compounds in the longan pericarp cv. Daw

unhydrolysis (A) and acid hydrolysis (B).

Q = quercetin aglycone

K = kaempferol aglycone

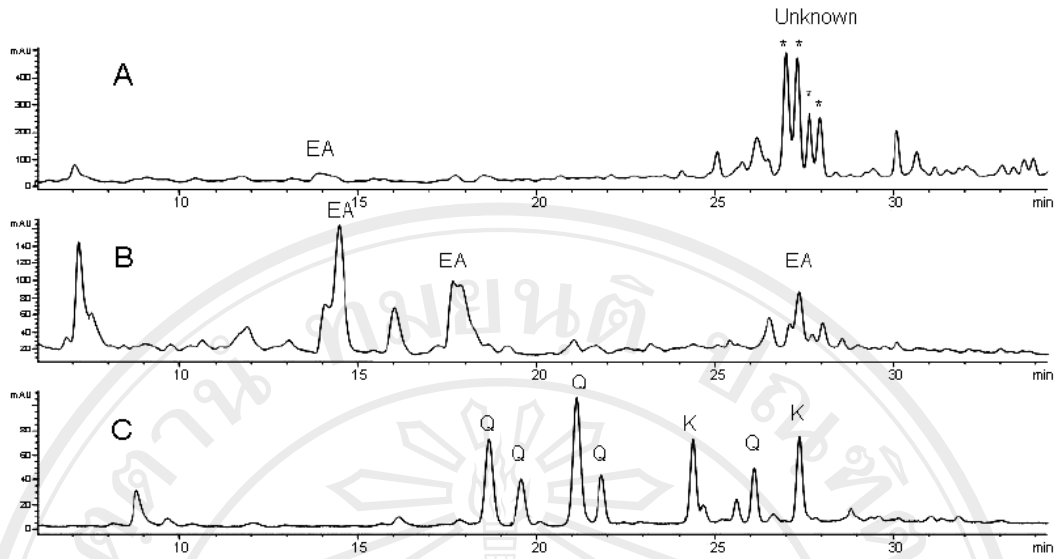


Figure 4.21 HPLC chromatograms at 330 nm of three P2 column fractions. Ellagic acid conjugates in chromatograms A and B are labeled by EA, and set of related phenolic unknown compounds are labeled with (*) in chromatogram A. The quercetin glycosides and kaempferol glycosides are labeled by Q and K in chromatogram C, respectively.

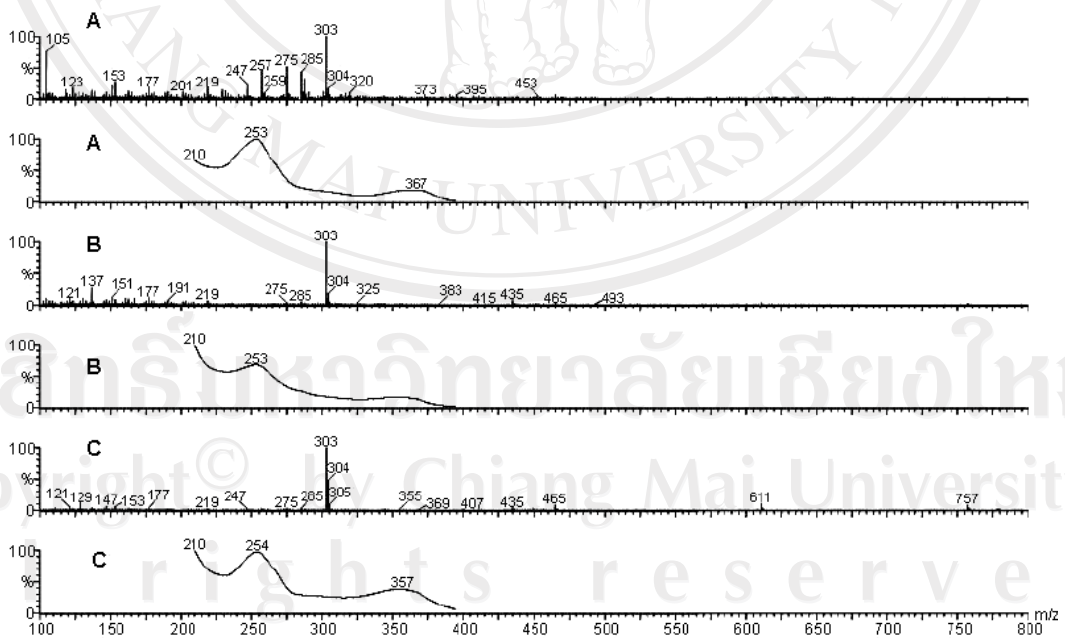


Figure 4.22 UV and mass spectra of the major ellagic acid conjugates detected in the freeze-dried normal longan pericarp.

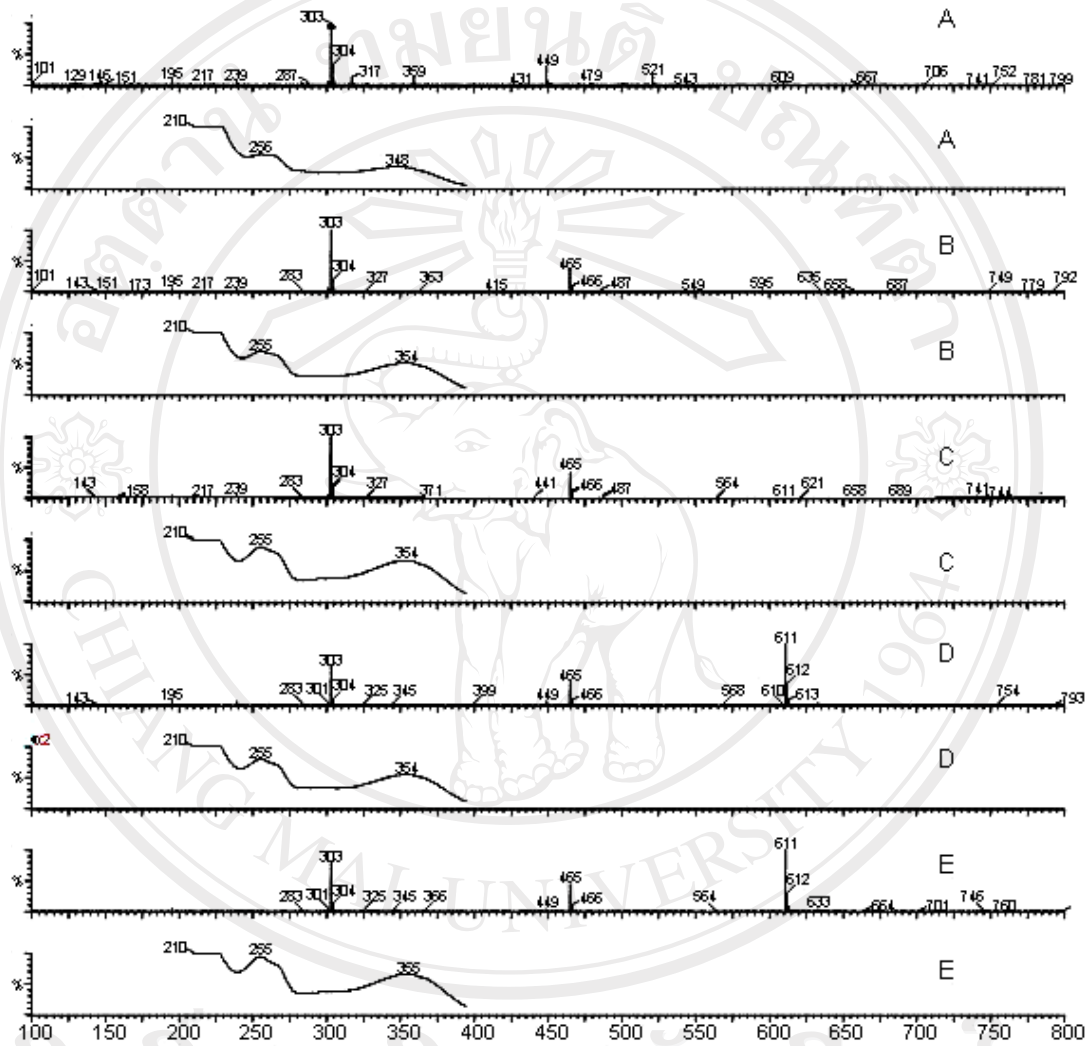


Figure 4.23 UV and mass spectra of quercetin glycosides in freeze-dried longan pericarp.

ลิขสิทธิ์มหาวิทยาลัยเชียงใหม่
 Copyright© by Chiang Mai University
 All rights reserved

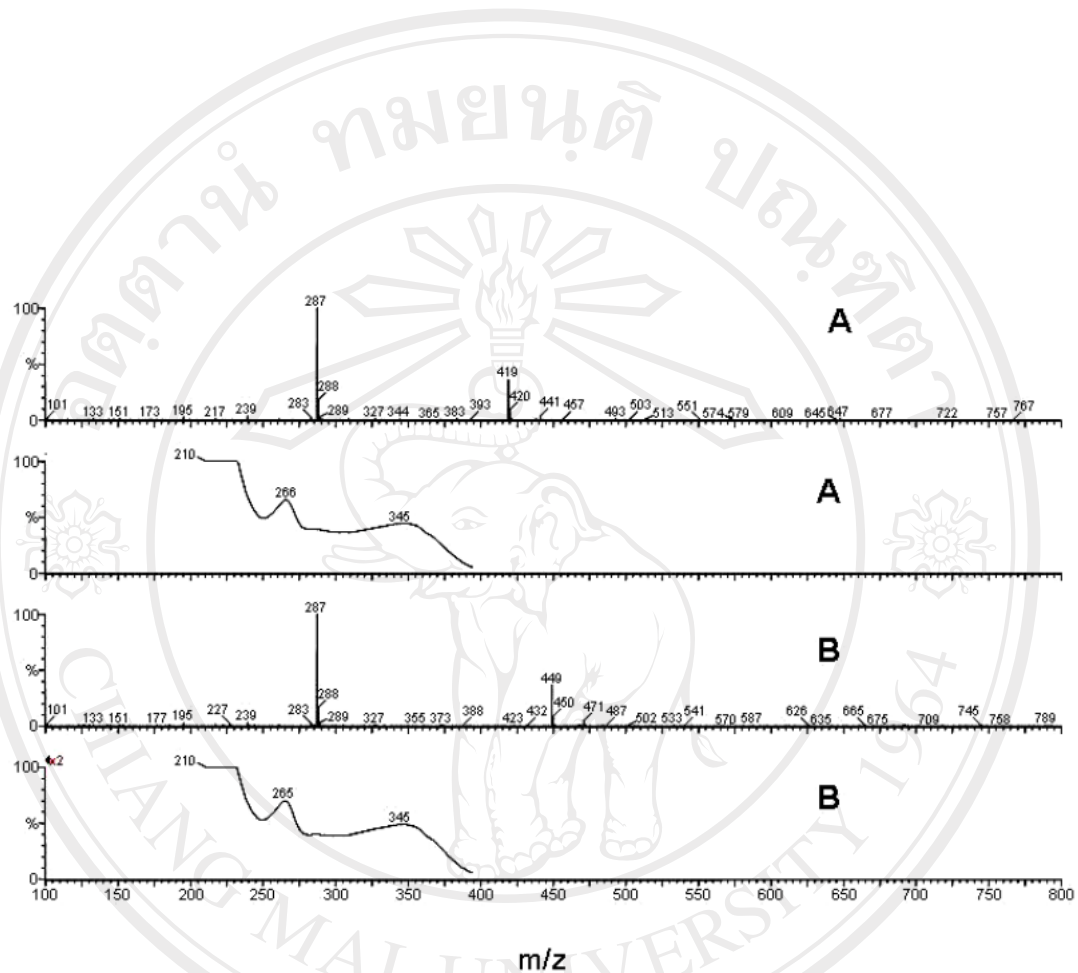


Figure 4.24 UV and mass spectra of 2 kaempferol glycosides in freeze dried longan pericarp.

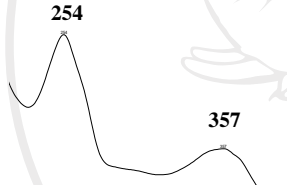
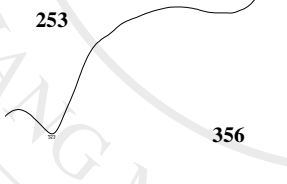
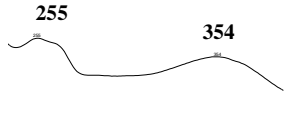
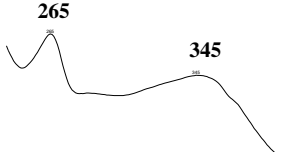
Table 4.6

Mass spectra of kaempferol glycosides in longan pericarp. Abbreviations are: K, kaempferol; glc, glucose; rha, rhamnose. A pentose is indicated by the neutral loss of 132 amu (150 amu-18 (H₂O)). The +Na adduct (+Na) is observed as a mass ion 22 amu above the protonated mass ion (M+H) +1. Neutral losses indicated by parentheses.

Elution time (min)	Molecular mass fragment	Possible structure
21.1	617(+Na)/595(M+H)+1/449(-146)/287(-162)	K + glc + rha
23.1	617(+Na)/595(M+H)+1/449(-146)/287(-162)	K + glc + rha

24.4	471(+Na)/449(M+H)+1/287(-162)	K + glc
26.1	441(+Na)/419(M+H)+1/287(-132)	K + pentose
28.7	455(+Na)/433(M+H)+1/287(-146)	K + rha

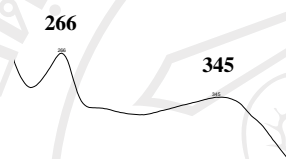
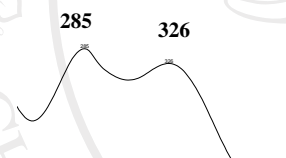
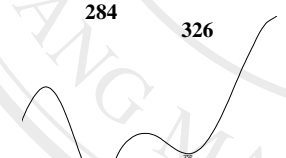
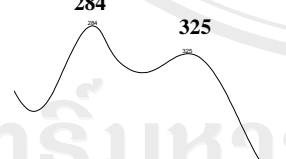
Table 4.7 The main class of phenolic compounds conjugates in freeze-dried longan pericarp was identified by HPLC-PDA-MS, including ellagic acid glycosides, quercetin glycosides, kaempferol glycosides and unknown compounds.

Elution time (min)	UV	MS fragment (Scan ES ⁺)	Possible structure
14.80		303 [M-H] ⁺ , 465 (+glu), 611(+rha), 757 (+rha)	Ellagic acid+glucose+ 2 rhamnose
15.08		303 [M-H] ⁺ , 435, 611, 757	Ellagic acid-pentose conjugate
20.37		303 [M-H] ⁺ , 465 (+glu), 611 (+rha)	Quercetin+glucose +rhamnose
21.38		303 [M-H] ⁺ , 465(+glu), 595, 741	Quercetin+glucose
24.28		287 [M-H] ⁺ , 449 (+glu)	Kaempferol+glucose
			

25.90

Quercetin+rhamnose

303[M-H]⁺, 449(+rha)**Table 4.7 (continued).**

Elution time (min)	UV	MS fragment	Possible structure
27.14		287 [M-H] ⁺ , 419	Kaempferol-pentose conjugate
26.92		177, 373, 535, 697	Unknown compound (UV absorbance 285, 326 nm)
27.25		137, 177, 327, 355, 535, 697	Unknown compound (UV absorbance 284, 326 nm)
27.48		137, 177, 337, 451, 535, 692	Unknown compound (UV absorbance 284, 325 nm)

4.5.2 Analysis of unknown compounds

The longan pericarp extracts contained a large number of compounds that belied easy structural analysis by HPLC-PDA-MS. A particularly interesting set of 4 compounds eluted between 26-28 minutes (Figure 4.21 A), and exhibited nearly identical UV and mass spectra. Further analysis was done on thin layer chromatography (TLC) and HPLC purified samples of these compounds. The three major compounds in this set of unknowns exhibited nearly

identical migration on TLC and were isolated to a single spot on analytical TLC (Figure 4.25). Although the recovered amounts were not sufficient for NMR analysis, there were sufficient amounts for further MS analysis and FTIR spectroscopy. Figure 4.26 showed the UV and MS of the 3 isolated compounds. The UV spectra were nearly identical, and were similar to UV spectra of hydroxycinnamates (Wolf, 1968). In the same manner, the MS of the three unknown compounds were nearly identical, each showing a protonated molecular weight of 697 m/z . Each also showed neutral losses [(697 amu-535 amu), and (535 amu-373 amu)] of two hexoses (possibly glucose), yielding the fragment ion at 373 m/z . A loss of water (-18 amu) from this latter ion yielded a fragment ion at 355 m/z . The remaining fragment ion at 177 m/z did not correspond to any of the common hydroxycinnamic acids, and additional information was obtained from the mass spectra.

When these compounds were analyzed by FTIR, the results confirmed the presence of glycosidic groups (ν_{OH} 3350 cm^{-1} , and complex ν_{C-O} vibrations between 1400-1050 cm^{-1}), and of phenyl rings (1515 cm^{-1}), and carbonyl substituents (1700, 1626, 1599 cm^{-1}). The FTIR spectrum of the unknown compound B was shown in Figure 4.27. Included in Figure 4.27 was the FTIR spectrum of a mixture of hydroxycinnamates previously isolated from orange pericarp molasses (Manthey, 2004). These latter compounds have been previously reported to constitute mainly ferulic and *p*-coumaric acid esters of neutral sugars and glucaric acids. Many similarities between the FTIR spectra of the unknown compound B and that of the mixture of hydroxycinnamates help support a preliminary classification of these compounds as hydroxycinnamates, containing glycosidic side groups. Hydroxycinnamic derivatives (HCD) derived from cinnamic acid and are essentially present as combined forms of the four basic molecules *p*-coumaric, caffeic, ferulic and sinapic acids (Macheix *et al.*, 1990). However in longan seed was found 12 unknown compounds and most likely ellagitannin (Soong and Barlow, 2005).



Figure 4.25

Analytical silica gel TLC of 3 related unknown compounds. The 3 main unknown compounds, A-C, were applied to 200 μm thickness. Analtech analytical TLC plates with fluorescence indicator. Visualization was made with UV light (365 nm), and with the application of a 5% H_2SO_4 in ethanol spray followed by heat. No spots in lanes A-C other than the unknown compounds were detected by either UV irradiation or by charring with H_2SO_4 and heat.

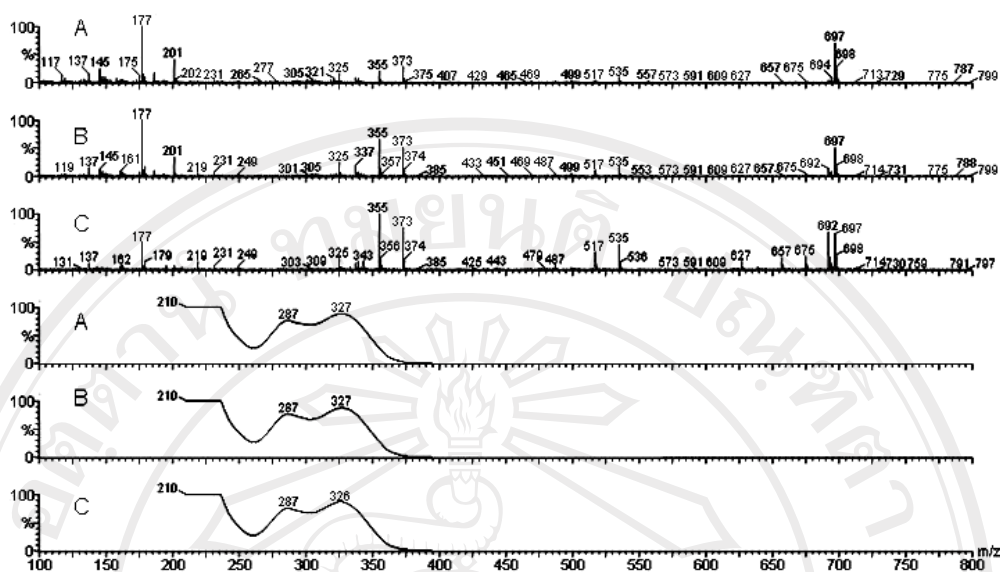


Figure 4.26

UV and mass spectra of 3 related unknown compounds. Mass spectra were recorded with an electrospray ionization cone voltage of +20 V.

4.5.3 Quantification of phenolic compounds in longan fruit pericarp

The major phenolic compounds in longan fruit pericarps were identified as quercetin glycosides, kaempferol glycosides, ellagic acid glycosides and complex of hydroxycinnamates. The phenolic compounds in cv. Daw were identified as ellagic acid, quercetin, kaempferol and complex of hydroxycinnamates (**Figure 4.28 A**) and in cv. Biew Kiew were identified as quercetin, kaempferol and complex of hydroxycinnamates while no ellagic acid was detected by LC-MS in this cultivar (**Figure 4.28 B**). However, only quercetin and kaempferol were quantified because of an ellagic acid showed peak overlaps in the chromatograms and also complex of hydroxycinnamates (**Figure 4.28**).

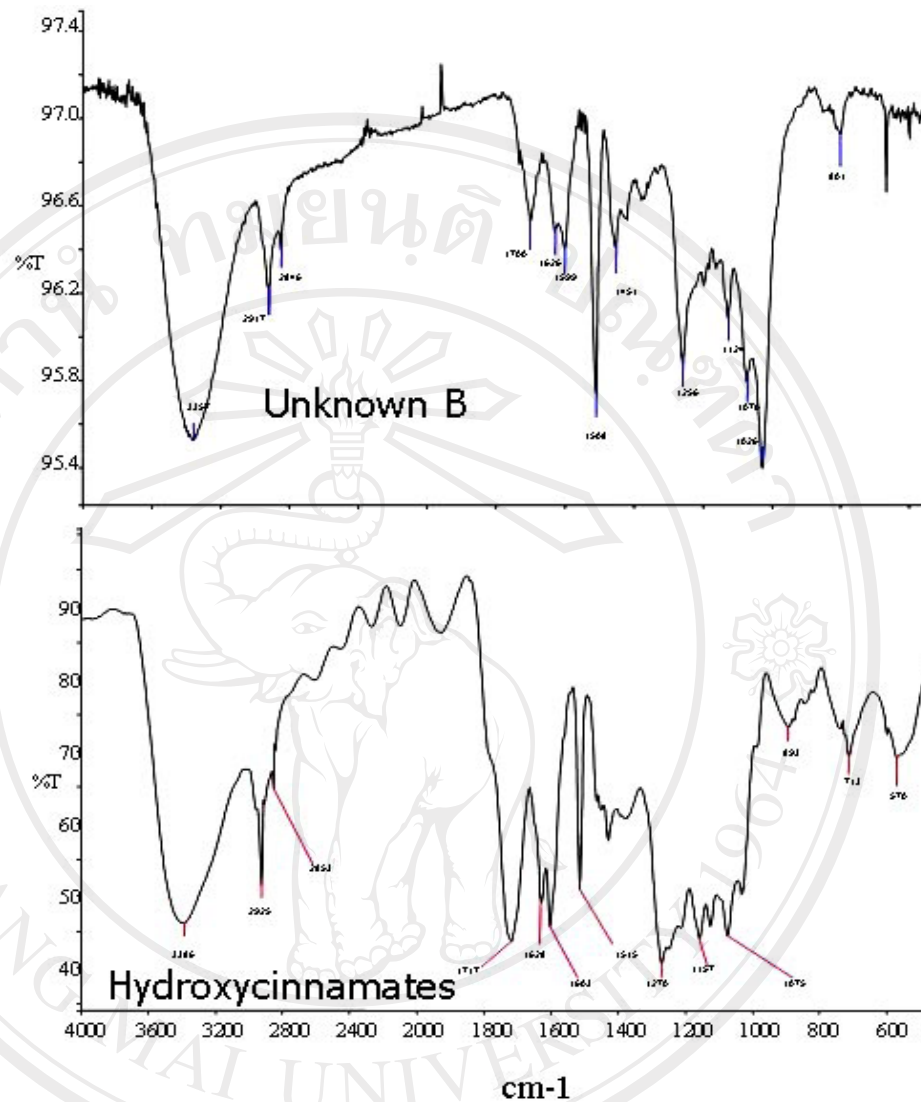


Figure 4.27

Fourier transform infrared spectra of unknown B (top) and citrus molasses hydroxycinnamates (bottom). Each spectrum is summations of 8 scans recorded with a Perkin Elmer (Norwalk, Conn.). Spectrum One FTIR spectrophotometer. Samples dissolved in ethanol were dried onto Real Crystal KBr IR card (International Crystal Laboratories, Garfield, NJ, USA) prior to the FTIR measurements.

Changes of identified phenolic compounds of longan fruit pericarps cv. Daw and Biew Kiew during chilling injury storage at 5°C decreased from 0.323 to 0.155 g and 0.302 to 0.064 g/100 g DW for quercetin and decreased from 0.111 to 0.057 g and 0.099 to 0.048 g/100 g DW for kaempferol, respectively (**Tables 4.8 and 4.9**). The results have demonstrated a linear correlation between quercetin and kaempferol contents of longan pericarp cv. Daw ($r^2 = 0.88$ and 0.70) and Biew Kiew ($r^2 = 0.93$ and 0.88), respectively during storage at 5°C for 14 days (**Figure 4.29**).

Rangkadilok *et al.* (2005) reported that ellagic acid in dried pericarp was 1-1.5 times higher than fresh pericarp. Gallic acid content was the highest in dried seed (0.8-2.3 mg/g DW) and in the dried seed was 5-10 times higher than fresh seed. However, fresh seed contained higher levels of ellagic acid (1.4-4.5 mg/g DW) than dried seed (1.4-2.5 mg/g DW). Pericarp and seed also contained corilagin at high levels while aril contained low levels (0.08-0.15 mg/g DW in dried aril). The highest corilagin content was found in dried seed (3.7-8.6 mg/g DW). Soong and Barlow (2005) reported that phenolic contents in longan seed were 23 mg/100 g of gallic acid and 156 mg/100 g of ellagic acid.

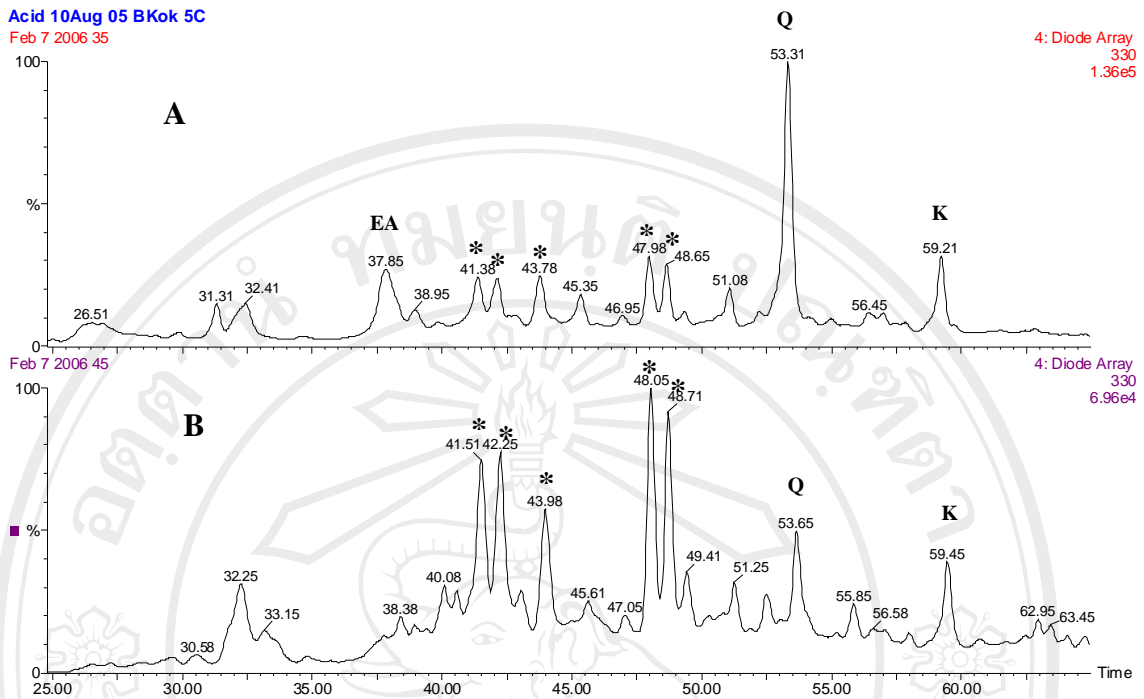


Figure 4.28 HPLC chromatograms at 330 nm of hydrolyzed phenolic compounds extracted from longan pericarps cv. Daw (A) and Biew Kiew (B).

EA = Ellagic acid

Q = Quercetin

K = Kaempferol

* = Complex of hydroxycinnamates

Table 4.8 Quercetin content¹ of freeze-dried longan pericarps cv. Daw and Biew Kiew during storage at 5 and 10°C.

Cultivars	Temp. (°C)	Days of storage*							
		0	2	4	6	8	10	12	14
Daw	5	0.323±0.001 ^a	0.253±0.001 ^b	0.231±0.001 ^c	0.208±0.000 ^b	0.206±0.001 ^b	0.181±0.001 ^b	0.179±0.000	0.155±0.001
	10	0.323±0.001 ^a	0.331±0.000 ^a	0.323±0.001 ^a	0.228±0.000 ^a	0.221±0.001 ^a	0.213±0.001 ^a	0.179±0.000	0.162±0.000
Biew Kiew	5	0.302±0.001 ^b	0.225±0.001 ^d	0.166±0.001 ^d	0.099±0.001 ^d	0.086±0.000 ^d	0.064±0.001 ^d		
	10	0.302±0.001 ^b	0.251±0.000 ^c	0.235±0.001 ^b	0.145±0.001 ^c	0.140±0.000 ^c	0.103±0.002 ^c		
LSD _{0.05}		0.0028	0.0019	0.0027	0.0016	0.0017	0.0025		
C.V. (%)		0.47	0.39	0.59	0.50	0.56	0.95		

¹Quercetin content (g/100g of dry weight).

*Means within the same column followed by different letters are significantly different at 95% ($P \leq 0.05$) level.

Data are mean values \pm SE.

Table 4.9 Kaempferol content¹ of freeze-dried longan pericarps cv. Daw and Biew Kiew during storage at 5 and 10°C.

Cultivars	Temp. (°C)	Days of storage*							
		0	2	4	6	8	10	12	14
Daw	5	0.111±0.005 ^a	0.086±0.001 ^b	0.070±0.000 ^b	0.067±0.000 ^b	0.066±0.001 ^b	0.070±0.000 ^b	0.063±0.001	0.057±0.000
	10	0.111±0.005 ^a	0.109±0.000 ^a	0.108±0.000 ^a	0.080±0.000 ^a	0.078±0.000 ^a	0.076±0.000 ^a	0.063±0.000	0.059±0.000
Biew Kiew	5	0.099±0.001 ^b	0.079±0.000 ^d	0.063±0.001 ^c	0.059±0.000 ^c	0.048±0.001 ^d	0.048±0.001 ^c		
	10	0.099±0.001 ^b	0.081±0.001 ^c	0.071±0.001 ^b	0.059±0.001 ^c	0.055±0.000 ^c	0.049±0.001 ^c		
LSD _{0.05}		0.0101	0.0016	0.0016	0.0014	0.0014	0.0016		
C.V. (%)		5.08	0.98	1.11	1.10	1.20	1.37		

¹Kaempferol content (g/100g of dry weight).

*Means within the same column followed by different letters are significantly different at 95% ($P \leq 0.05$) level.

Data are mean values \pm SE.

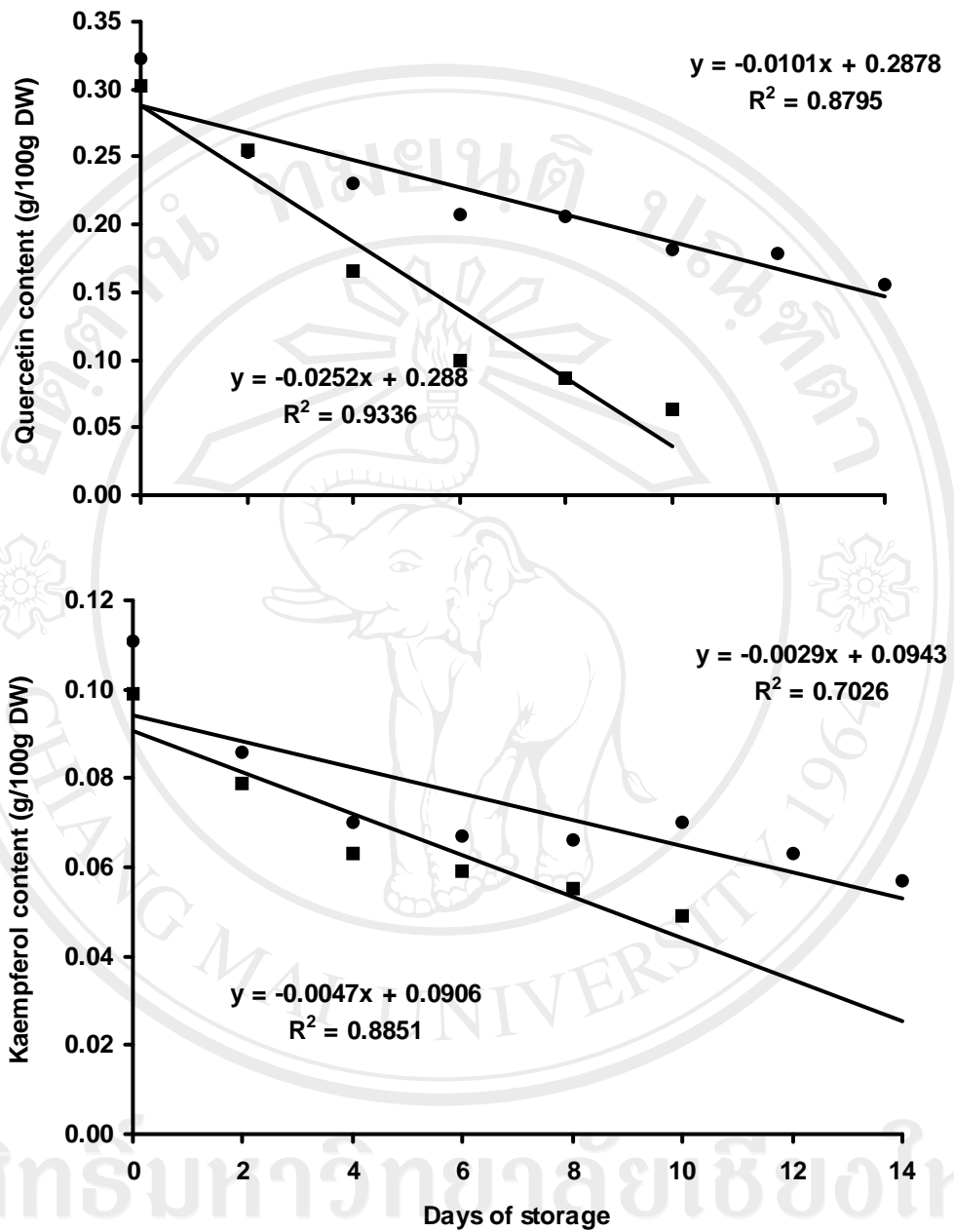


Figure 4.29 Correlation between quercetin and kaempferol contents of longan pericarp cv. Daw and Biew Kiew during storage at 5°C.
 ● Daw ■ BK

4.6 Quantification of other components of normal and chilling injured longan fruit pericarps cv. Daw and Biew Kiew

The cell wall components, total dietary fiber (TDF), pectin and lignin of freeze-dried normal and chilling injured longan fruit pericarps cv. Daw and Biew Kiew were studied. The cell wall components of longan fruit pericarp cv. Daw were similar to cv. Biew Kiew. The cell wall components of normal longan fruit pericarp cv. Daw were consisted of TDF 7.26 g, pectin 0.89 g and lignin 0.019 g/100g DW. Cell wall composition of longan fruit pericarp cv. Biew Kiew were consisted of TDF 7.28 g, pectin 0.085 g and lignin 0.019 g/ 100g DW (**Table 4.10**). The longan fruit pericarp in cv. Biew Kiew showed a similar trend of TDF, pectin and lignin contents changes during storage at 5°C (**Figure 4.30**). The cell wall component changes of longan pericarp cv. Daw were consisted of TDF ranged from 6.95 to 7.26 g/100 g, pectin ranged from 0.87 to 0.97 g and lignin ranged from 0.019 to 0.021 g/100 g DW. In addition, the cell wall components changes of longan pericarp cv. Biew Kiew were consisted of TDF ranged from 7.28 to 7.52 g, pectin ranged from 0.61 to 0.85 g and lignin ranged from 0.019 to 0.024 g/100 g DW. These results did not demonstrated any clearly distinguishable differences between CI and cell wall components (in cases of TDF, pectin and lignin contents) in longan fruit pericarp of both cultivars. However, the overall of pericarp components showed TDF slightly increased, pectin decreased and slightly change in lignin content during storage. This result agree with the previous work reported that pectin decreased in chilling injured kiwifruit (Bauchot *et al.*, 1999) and peach fruit (Manganaris *et al.*, 2006).

Table 4.10 TDF, pectin and lignin contents of normal and chilling injured longan fruit pericarps cv. Daw and Biew Kiew during storage at 5°C.

Cell wall component (g/100 g DW)	Cultivar	Chilling injury level			
		1	2	3	4
TDF	Daw	7.26±0.02	7.08±0.03	7.45±0.02	6.95±0.05
	Biew Kiew	7.28±0.03	7.48±0.03	7.50±0.02	7.52±0.03
Pectin	Daw	0.89±0.01	0.87±0.02	0.96±0.02	0.97±0.02
	Biew Kiew	0.85±0.02	0.76±0.02	0.71±0.02	0.61±0.03
Lignin	Daw	0.019±0.0	0.019±0.0	0.200±0.0	0.210±0.0
	Biew Kiew	0.019±0.0	0.021±0.0	0.021±0.0	0.024±0.0

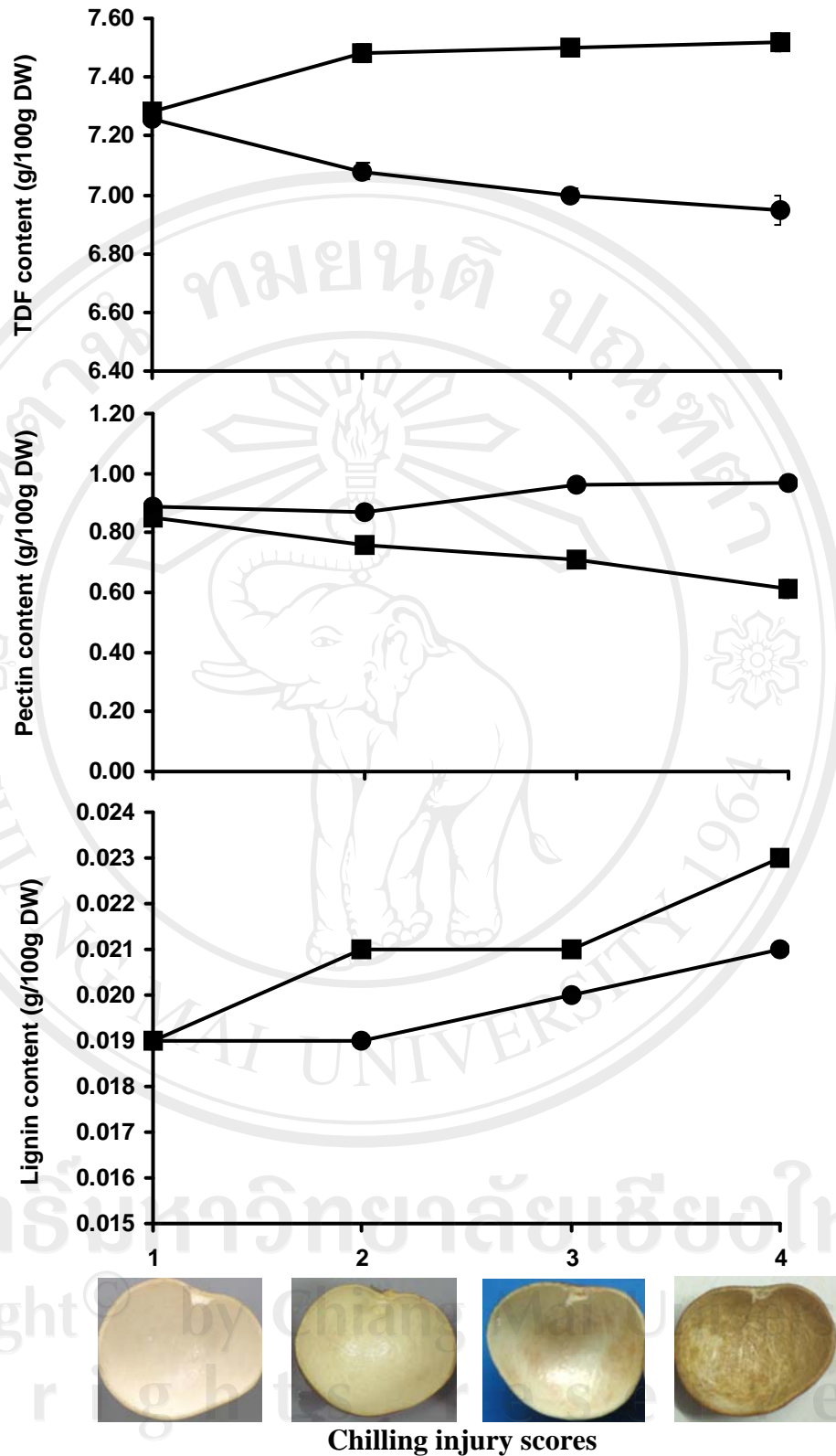


Figure 4.30 TDF, pectin and lignin contents of longan pericarps cv. Daw and Biew Kiew between chilling injury score levels during storage at 5°C.

● Daw ■ BK